USE OF AN AIRBORNE FRAUNHOFER LINE DISCRIMINATOR FOR THE DETECTION OF SOLAR STIMULATED LUMINESCENCE

by

Robert D. Watson[1/] and William R. Hemphill[2/]
U. S. Geological Survey

- 1976 -
U. S. Geological Survey
OPEN FILE REPORT 76202

1/ Flagstaff, Arizona
2/ Reston, Virginia

Supported by the
National Aeronautics and Space Administration's
Advanced Applications Flight Experiments and
Supporting Research and Technology Programs
and the
Department of the Interior's
Earth Resources Observation Systems Program

CONTENTS

ILLUSTRATIONS

Figure 10: Dye concentration patterns based on unreduced FLD readings made on eight runs during late morning (11:07-11:34) June 13, 1974. The three dyes were released at points 152, 229, and 304 metres (500, 750, and 1000 feet) from shore between 10:26 and 10:28 a.m. Numbered circles and triangles are anchored buoys and on-shore reference points.

Figure 11. Luminescence versus dye concentration obtained during calibration of the Fraunhofer line discriminator. The three curves were obtained by varying the concentration of each dye separately in a tank containing 1/2 metre of water. Luminescence counts were measured with the FLD suspended above the tank. Note that the abscissa has been reduced by a factor of 5.0 for Uranine B.

Figure 12. Stripple pattern shows area of figure 13. (Modified from Huff (1963).

Figure 13. Distribution of copper and location of sample trees growing in background and anomalous oils (modified from Huff (1963).

Figure 14. Excitation spectra of Pinus ponderosa needles from geochemically anomalous and background areas, Malachite Mine, Jefferson County, Colorado, as measured with a laboratory fluorescence spectrometer (source-detector corrected only). Integration of the area under each excitation spectrum permits comparison with the excitation spectra of a rhodamine WT standard.

Figure 15. Relative luminescence of twigs from seven trees growing in a geochemically background area, Malachite Mine, Jefferson County, Colorado, 107.2 $\pm$ 9.6 counts. Mean and standard deviation of relative luminescence are measured in reference to nonluminescent gray-card standard (18 percent reflectance)

Figure 16. Relative luminescence of twigs from seven trees growing in a geochemically anomalous area, Malachite Mine, Jefferson County, Colorado, 90 ± 19.6 counts. Mean and standard deviation of relative luminescence are measured in reference to nonluminescent gray-card standard (18 percent reflectance).

Figure 17. Temporal luminescence of Pinus ponderosa and meteorological parameters. Maximum luminescence contrast between stressed and non-stressed trees tends to occur during periods of minimum cloud cover.

Figure 18. Temporal luminescence of Pinus ponderosa and meteorological parameters. Minimum luminescence contrast between stressed and non-stressed trees tends to occur during periods of maximum cloud cover.

Figure 19. Temporal luminescence of Pinus ponderosa and meteorological parameters. Luminescence contrast of stressed and non-stressed trees do not correlate with cloud cover conditions cited in Figure 17 and 18.

Figure 20. Location of geochemically anomalous and background trees in the Alpine Mill area, about 17 km southeast of Gardnerville, Douglas County, Nevada. Background trees are arbitrarily denoted as those containing 70 ppm molybdenum or less.

Figure 21. Linear regressive analysis correlating FLD luminescence counts for specific trees with molybdenum concentrations from 20 to 300 ppm.

Figure 22. Geologic map of part of the Sespe Creek area showing location of the helicopter traverse and helicopter hovers (A through D).

TABLES

Table 8. Reflectance, FLD counts, and luminescence in terms of rhodamine WT equivalency (source-detector, solar, and depth corrected) of phosphate, gypsum, and background reference materials. Field FLD measurements were performed in November, 1964.

Table 9. Reflectance, FLD counts, and luminescence in terms of rhodamine WT equivalency of phosphate, gypsum and background materials. Field FLD measurements were performed May 8, 1975.

Table 10. FLD counts and luminescence in terms of rhodamine WT equivalency of associated phosphate and gypsum materials in the Lakeland, Florida area.

Table 11. Integrated excitation intensity of crude oils at specific Fraunhofer wavelengths in terms of equivalency with rhodamine WT.

Table 12. Integrated excitation intensity of refined oils at specific Fraunhofer wavelengths in terms of equivalency with rhodamine WT.

Table 13. Integrated excitation intensity of crude oils and oil films at six Fraunhofer wavelengths in terms of rhodamine WT equivalency.

Table 14. Luminescence at 486.1 nm of sulfurized liquor and background materials in the vicinity of the Buckeye Cellulose plant, Foley, Florida in terms of MPF-3 rhodamine WT equivalency, FLD counts, and FLD rhodamine WT equivalency.

Table 15. Equivalent tannic acid in parts per million for waters in the vicinity of the Buckeye Cellulose plant, Foley, Florida.

Table 16. Luminescence of samples of phosphate processing effluent at six Fraunhofer lines in terms of rhodamine WT equivalency (source-detector and solar corrected; depth corrected to 4 cm). Effluent samples were collected from processing plants west of Mulberry Florida. Reference samples were collected from rivers several tons of kilometres outside the phosphate area.

Table 17. Measurement of luminescence effluents and associated materials at a phosphate processing plant near Lakeland, Florida. Luminescence is presented in terms of FLD counts as well as rhodamine WT equivalences (source-detector, solar, and depth corrected) derived from both FLD and MPF-3 measurements.

Table 18. Luminescence measured from a helicopter with the FLD compared with laboratory predicted values measured with the MPF-3 fluorescence spectrometer (source-detector, solar, and depth corrected).

Use of an airborne Fraunhofer line discriminator for the detection of solar stimulated luminescence

by

Robert D. Watson[1/] and William R. Hemphill[2/]
U.S. Geological Survey

ABSTRACT

Luminescence is the property of some materials to emit light when excited by external stimuli such as ultraviolet or visible light or by chemical or mechanical action. The Fraunhofer line discriminator (FLD) is an airborne electro-optical device which operates as a non-imaging radiometer and permits detection of solar stimulated luminescence several orders of magnitude below the intensity detectable with the human eye. A prototype FLD, used in 1969 to monitor the dynamics of water currents in the San Francisco area, was sensitive to the luminescent dye, rhodamine WT, in concentrations of less than 5 parts per billion.

Airborne tests of a redesigned FLD, featuring an order of magnitude improvement in sensitivity, permitted measurement of differences in the luminescence of trees growing in soils containing geochemically anomalous concentrations of copper (near Denver, Colorado) and molybdenum (near Gard - nerville, Nevada) from trees growing in background areas nearby. In the tests near Denver, luminescence-contrast between stressed and non-stressed trees tended to be greater during periods when cloud cover was 10 percent or less; in most cases, contrast was insignificant when cloud cover exceeded 10 percent. In other airborne tests, the FLD distinguished luminescing phosphate rock and gypsum from sandstone and siltstone near Pine Mountain, California;

[1/] Flagstaff, Arizona

[2/] Reston, Virginia

dispersal of oil in a natural seep from uncontaminated sea water in the Santa Barbara Channel; cattle feed lot and municiple sewage effluents near Denver; and paper and phosphate processing effluents in eastern and central Florida.

Procedures employing a laboratory fluorescence spectrometer permit prediction of the detectivity with an FLD prior to monitoring an airborne test. Luminescence spectra of the material are corrected for wavelength variation in spectrometer source, detector sensitivity, and solar illumination. By comparing these results with the luminescence of a rhodamine WT dye standard, the luminescence of the material may be expressed in terms of rhodamine dye equivalency at the wavelength of several Fraunhofer lines. The FLD detectivity may be assessed at each Fraunhofer line, and the optimum line for field observation of the material may be selected.

Future work will include the integration of the FLD with a line scan imaging system in order to assess the contribution of two-dimensional spatial resolution to the interpretability and usefulness of luminescence data. It should also include 1) investigation of luminescence polarization of some materials, particularly metal stressed plants, 2) an assessment of the use of pulsed lasers to stimulate phosphorescence decay time in the nanosecond and microsecond ranges; and 3) a study to determine the feasibility of conducting an FLD experiment from the Space Shuttle or other spacecraft.

1. INTRODUCTION

Laboratory and field study of the measurement and interpretation of luminescent materials began in 1964, with experimental work using an active ultraviolet imaging system (Hemphill and others, 1965; Hemphill and Carnahan, 1965). This work led to the development of a prototype Fraunhofer line discriminator (FLD); an airborne remote sensing tool for measuring luminescence. The FLD was designed to operate on the Fraunhofer line depth principal (Kozyrev, 1956; Grainer and Ring, 1962) which uses the sun as an excitation source and permits detection of luminescing materials under daylight conditions. Experiments with the instrument showed that selected materials, such as luminescing tracer dyes, could be detected in very small quantities (Hemphill and others, 1969; Stoertz and others, 1969). For example, rhodamine WT dye was detected in the Pacific Ocean west of the Golden Gate in California in concentrations of less than 5.0 ppb (parts per billion). Attempts to measure the luminescence of other materials were not successful because 1) the prototype FLD operated at 589.0 nanometres (nm), the wavelength of the sodium D Fraunhofer line, and many materials luminesce at other wavelengths; and 2) the sensitivity was an order of magnitude less than required for detection of some of these materials.

In order to predict optimum wavelength and sensitivity requirements for detection of materials other than rhodamine WT, luminescence of a variety of materials was measured with a laboratory fluorescence spectrometer in terms of rhodamine WT, used as a laboratory standard. These results, coupled with those obtained with the prototype FLD were used as a basis for engineering a redesigned FLD with an order of magnitude increased sensitivity.

This redesigned model, built by the Perkin Elmer Corporation[1/] operates at three discrete Fraunhofer lines, hydrogen β at 486.1 nm, sodium D at 589.0 nm, and hydrogen α at 656.3 nm and has the sensitivity to detect rhodamine WT dye in concentrations as low as 0.1 parts per billion (ppb) in 1/2 (m) of water at 20° Celcius (C). An additional system built by Isomet Electronics uses a tunable acoustical optical filter which permits tuning to an accuracy of less than 0.5 nm with an average bandwidth of less than 0.1 nm. The sensitivity of this instrument is approximately an order of magnitude less than the Perkin Elmer FLD.

The basic approach to the problem of accurate measurement of luminescence both in the laboratory with a laboratory spectrometer and in the field with the redesigned model FLD is detailed in the following pages. The objective of this report is 1) to present the results of laboratory and field measurement of luminescence of natural materials in support of the design, development, and field testing of the redesigned FLD; 2) to demonstrate how the laboratory quantification of luminescence can be used to predict and interpret field measurements with the FLD; 3) to compare field results with design specifications of the redesigned FLD; and 4) to describe modifications to calibration techniques and operational procedures which evolved during field tests.

Luminescent materials reported herein include oils (bulk and thin film, both crude and refined), artificial dyes, phosphate rock and gypsum, phosphate processing plant effluent, vegetation (geochemically stressed versus non-stressed), lignin sulfonates, and selected industrial and residential pollutants.

[1/] Use of trade names in this paper is for description purposes only and does not constitute an endorsement of the product by the U.S. Geological Survey.

Design and development of the prototype FLD, and operational evaluation of its performance was jointly supported by the U.S. Geological Survey and by the National Aeronautics and Space Administration (NASA) Manned Spacecraft Center (renamed Johnson Space Center) through NASA's Supporting Research and Technology (SR & T) funds. Since 1971, development of the redesigned FLD by the Perkin-Elmer Corporation, as well as associated laboratory and field studies, has been supported by both the Earth Resources Observational Systems (EROS) Program of the Department of the Interior and the Advanced Applications Flight Experiments (AAFE) Program of NASA (NASA order L-58,514). Development of the FLD by Isomet Electronics was supported by NASA's Supporting Research and Technology (SR & T) Program.

2. FRAUNHOFER LINE DEPTH METHOD OF MEASURING LUMINESCENCE

Fraunhofer lines are dark lines in the solar spectrum caused by selective absorption of light by gases in the relatively cool upper part of the solar atmosphere. Line widths range from less than 0.01 nm to several tenths of a nanometer, and the central intensity of some lines is less than 10 percent of the adjacent continuum. The lines are sharpest, deepest, and most numerous in the near ultraviolet, visible, and near infrared regions of the electromagnetic spectrum.

The Fraunhofer line-depth method of measuring luminescence involves observing a selected Fraunhofer line in the solar spectrum, and measuring the ratio of the central intensity of the line to a convenient point on the continuum a few tenths nanometer distant; this ratio is compared with a similar ratio of a conjugate spectrum reflected from a material that is suspected to luminesce. Both ratios normally are identical, but luminescence is indicated where the reflected ratio exceeds the solar ratio. Reflectivity differences between the central intensity of the Fraunhofer line and the adjacent continuum can generally be ignored because variation of reflectivity with wavelengths is negligible for most materials over spectral ranges of only a few tenths nanometer.

Figure 1a shows an idealized Fraunhofer line observed in the solar spectrum directly, which may be expressed as the ratio R_s,

$$R_s = \frac{b}{a} \qquad (1)$$

where

b = central intensity

a = adjacent continuum

The same Fraunhofer line is given in Figure 1b, in a spectrum reflected from a nonluminescing material. The ratio of the line depth in the spectrum reflected by the material is

$$R_m = \frac{\rho b}{\rho a} = R_s. \qquad (2)$$

where

ρ = reflectance.

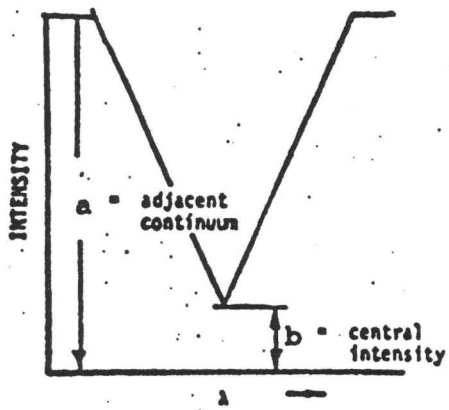

Figure 1a - Line profile in the solar spectrum observed directly

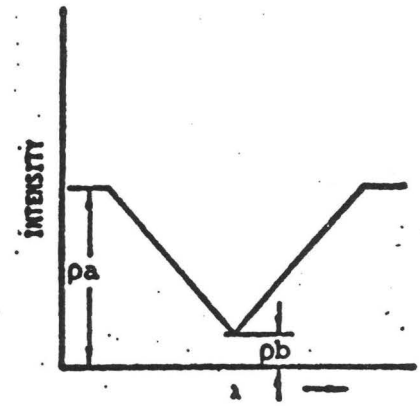

Figure 1b - Line profile in the solar spectrum reflected from nonluminescing materials

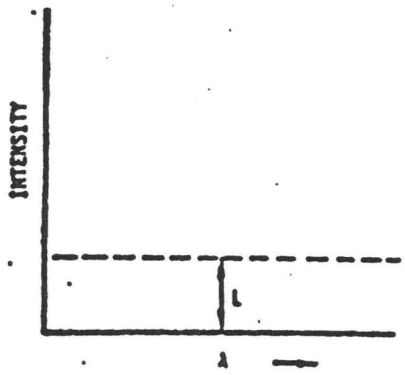

Figure 1c - Luminescence contribution as a nonvariable with wavelength

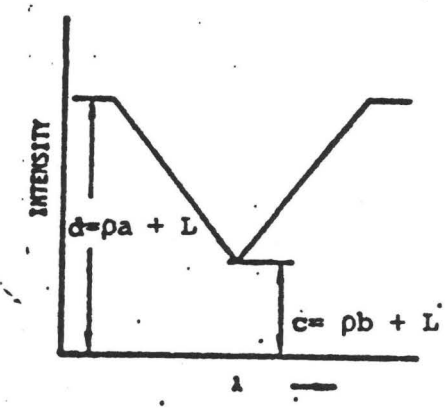

Figure 1d - Line profile of material containing both reflected and luminescent components

Figure 1c illustrates the luminescence component, L. Because many materials exhibit broad-band luminescence, commonly half-widths of several nanometers, the luminescence contribution, L shown in figure 1c may be assumed to be constant across the width of one Fraunhofer line.

Figure 1d shows the line profile of a material containing both reflected and luminescing components. Since the luminescence component is assumed to contribute equally to both the central intensity and the adjacent continuum,

$$d = \rho a + L \tag{3}$$

$$c = \rho b + L \tag{4}$$

$$R_m = \frac{\rho b + L}{\rho a + L} = \frac{c}{d} \; ; \; R_m > R_s \tag{5}$$

The difference between R_m and R_s is a measure of the amount of luminescence. The luminescence component may be measured in terms of the continuum component level, and expressed as a luminescence coefficient by

$$\xi = \frac{L}{a} \tag{6}$$

leading to

$$L = \xi a \tag{7}$$

where

ξ = luminescence coefficient

L = luminescence

a = continuum component level.

Substituting equation 7 into equations 3 and 4

$$d = \rho a + \xi a \tag{8}$$

$$c = \rho b + \xi a \tag{9}$$

These two equations can be solved to determine the two unknowns ρ and ξ.

Multiplying equation 8 by b, and equation 9 by a, yields

$$bd = \rho ab + \xi ab \tag{10}$$

$$ac = \rho ab + \xi a^2 \tag{11}$$

Subtracting equation 10 from equation 11

$$ac - bd = \xi a(a-b) \tag{12}$$

Solving for ξ:

$$\xi = \frac{ac - bd}{a(a-b)} \tag{13}$$

$$\xi = \frac{1}{a-b}\left[c - \frac{bd}{a}\right] \tag{14}$$

Equation 14 is useful because ρ and L are eliminated, and the expression of ξ is independent of incident solar flux.

3. LABORATORY PREDICTION OF THE FRAUNHOFER LINE DETECTIVITY OF LUMINESCENT MATERIALS

In order to assess the sensitivity required to detect luminescing materials, Hemphill and Stoertz (1971) and Watson and others (1973, 1974) used a laboratory fluorescence spectrometer (Figure 2) to quantify the luminescence

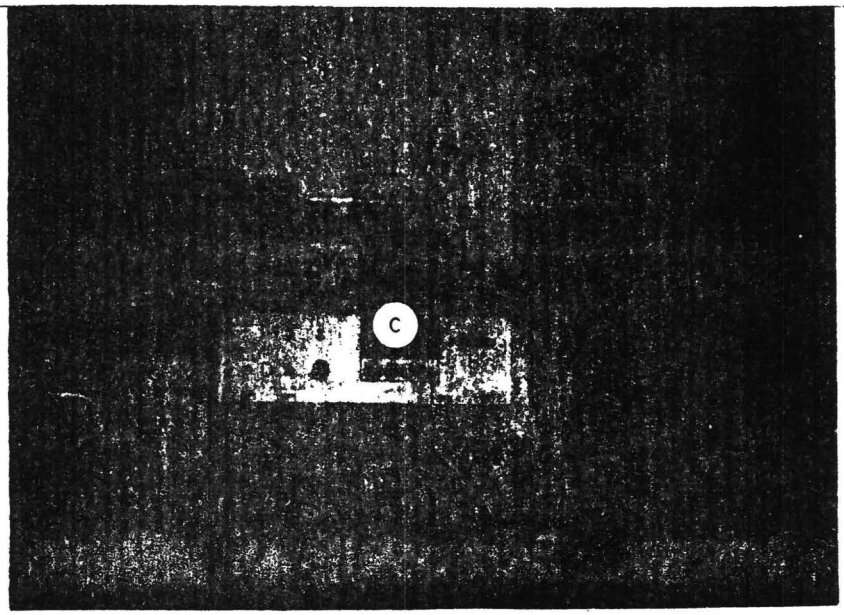

Figure 2. Laboratory fluorescence spectrometer. Source (A), excitation monochromator (B), sample compartment (C), emission monochromator (D), corrected spectra attachment (E), and recorder (F).

intensity of materials at six Fraunhofer lines (396.8, 442.7, 486.1, 518.4, 589.0, and 656.3 nm) in terms of equivalent luminescence of specific concentrations of rhodamine dye. The spectrometer was operated so as to produce excitation spectra; that is, the excitation monochromator was scanned while the emission monochromator was stationary at the wavelength of a specific Fraunhofer line. This arrangement provided a system in the laboratory analogous to an FLD in the field, where the broadband excitation of the sun produces an emission in a luminescent material, the intensity of

which is monitored at one or more Fraunhofer lines. The spectrometer, equipped with a corrected spectra attachment, automatically adjusted for the wavelength dependence of the source and detector, and produced a corrected distribution of excitation intensity.

In the front surface mode, solid samples, or liquid or powdered samples in a centimetre quartz cell, were so positioned in the sample compartment that both excitation and emission were through the front surface of the sample. Light from the excitation monochromator illuminated the sample surface at an angle of approximately 30° to the normal, and luminescence from the sample surface was directed in a narrow solid angle (centered at 90° from the incident beam) into the emission monochromator and onto the detector. In the right angle mode, light from the excitation monochromator passed through the sample cell, with resulting luminescence measured at right angles to the incident beam.

To relate all luminescence spectra to one set of conditions, rhodamine WT was used as the reference "standard" prior to each measurement. When the area under the curve of the excitation spectra of the sample was compared to the area under the curve for rhodamine WT dye (at a specific dye concentration), a relative equivalent rhodamine WT concentration was obtained. For example, a sample having an integrated excitation intensity of 50 was compared to a rhodamine WT concentration of 10 ppb, which also has an integrated excitation intensity of 50; the sample is said to have had an equivalent luminescence of 10 ppb rhodamine WT. This standardization makes it possible to correct for instrument response variations during measurement and to assess results achieved in the laboratory in terms of whether or not the same material in the field would be within the sensitivity range of an airborne FLD.

Self-absorption of luminescence intensity of rhodamine WT dye has increasingly important effects as the concentration increases. Figure 3 shows the self-absorption effect of rhodamine WT Dye where measured in both front surface and right angle modes. Because both front surface and right angle modes exhibit equal luminescence intensity at 1200 ppb, this concentration is used as a basis for the rhodamine WT standard in the following discussion.

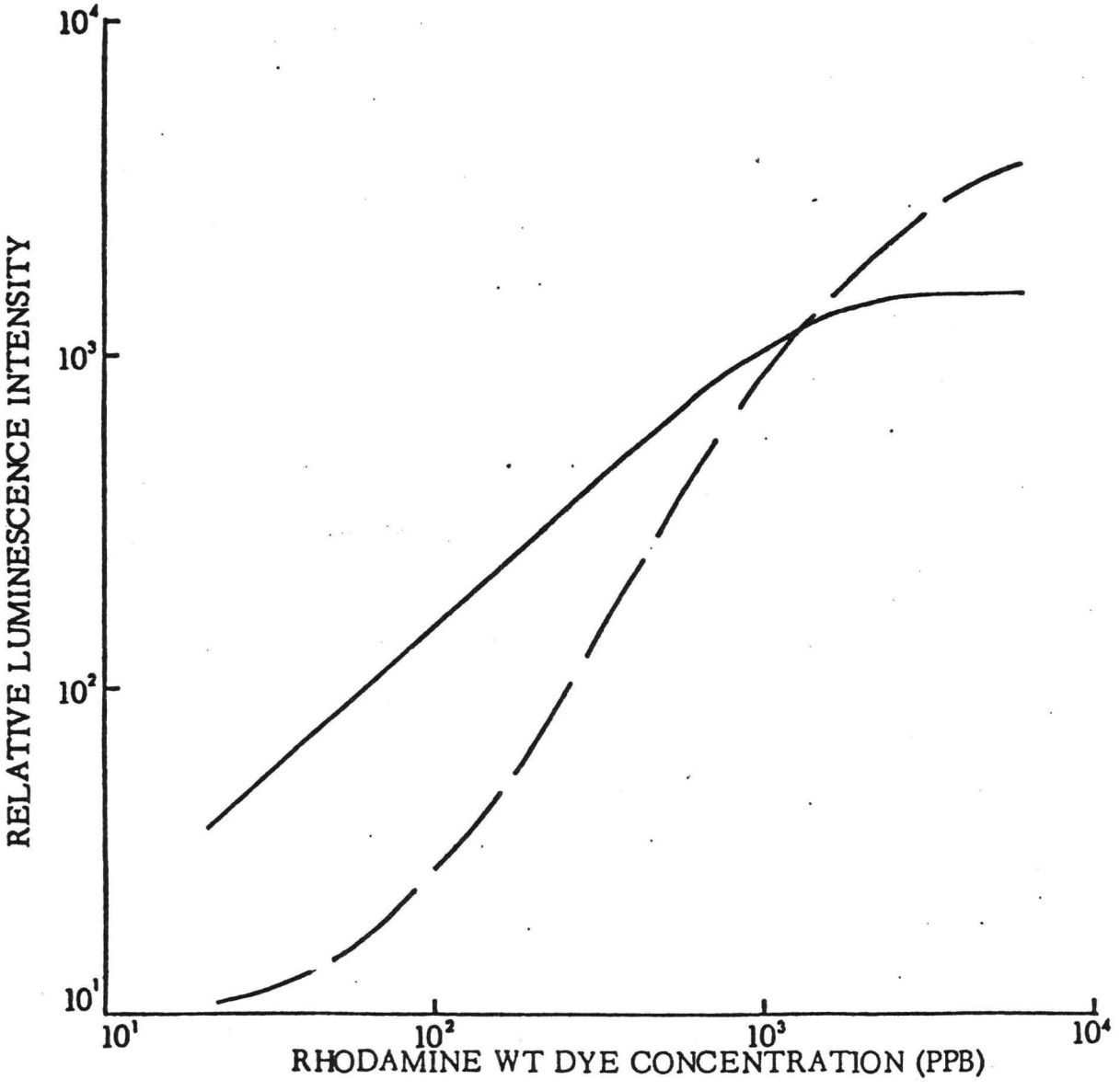

Figure 3. Relative luminescence intensity of rhodamine WT dye versus concentration as measured in both the front surface (solid line) and 90° or right angle modes (dashed line).

To obtain the same wavelength and intensity dependence of luminescence in the laboratory as would be observed in an FLD measurement, the source-detector corrected spectra must be convoluted with the spectral intensity of total solar radiation (direct sunlight plus diffuse skylight). Although direct sunlight and diffuse skylight vary diurnally and seasonally, the solar-corrected spectra presented by Watson, et al. (1973) are referenced to a standard set of conditions, as measured by Luckiesh (1946) in Cleveland, Ohio:

- ° airmass . 2.0
- ° solar constant = 1.9 cal cm^{-2} min^{-1} with diffuse radiation for a typical midday,
- ° midsummer clear weather.

A further correction is required when adjusting the standard of rhodamine dye as measured in a centimetre quartz cell in the spectrometer to that measured in the field in a half metre of water by the FLD. Measurements indicate that self-absorption of light emitted by rhodamine WT at the sodium line (589 nm) is negligible at low dye concentrations, but that the attenuation by particulates can be significant.

Equation 15 describes the emission of solar-stimulated luminescence $L(\lambda_F)$ in a Fraunhofer line at a wavelength λ_F from a solution of depth x, where absorption obeys the well known exponential relationship and luminescence is emitted uniformly in all directions:

$$L(\lambda_F) = \frac{1}{2\pi} \int_{\text{surface}}^{x} \int^{\Delta\lambda} I_{o\lambda} \cdot \exp(-\alpha_\lambda . x) \cdot Q_\lambda \cdot \exp(-\alpha_{\lambda F} . x) . d\lambda \, . dx$$

where $I_{o\lambda}$ = spectral solar radiation,

α_λ = measured attenuation coefficient of the solution at wavelength λ,

Q_λ = measured quantum efficiency of the solution (fraction of photons emitted at λ_F to those absorbed in $\Delta\lambda$),

$\Delta\lambda$ = wavelength band of excitation in the solar spectrum,

and $\alpha_{\lambda F}$ = measured attenuation coefficient of the solution at the emission wavelength λ_F.

For rhodamine WT dye in water, Q_λ represents the quantum efficiency of the dye (the water is assumed nonluminescent). $\alpha_{\lambda F}$ is the attenuation of the solution at an emission wavelength of 589.0 nm, and $\Delta\lambda$ is the wavelength band of excitation from 440 to 580 nm.

Using equation 15 and the attenuation coefficients shown in figure 4

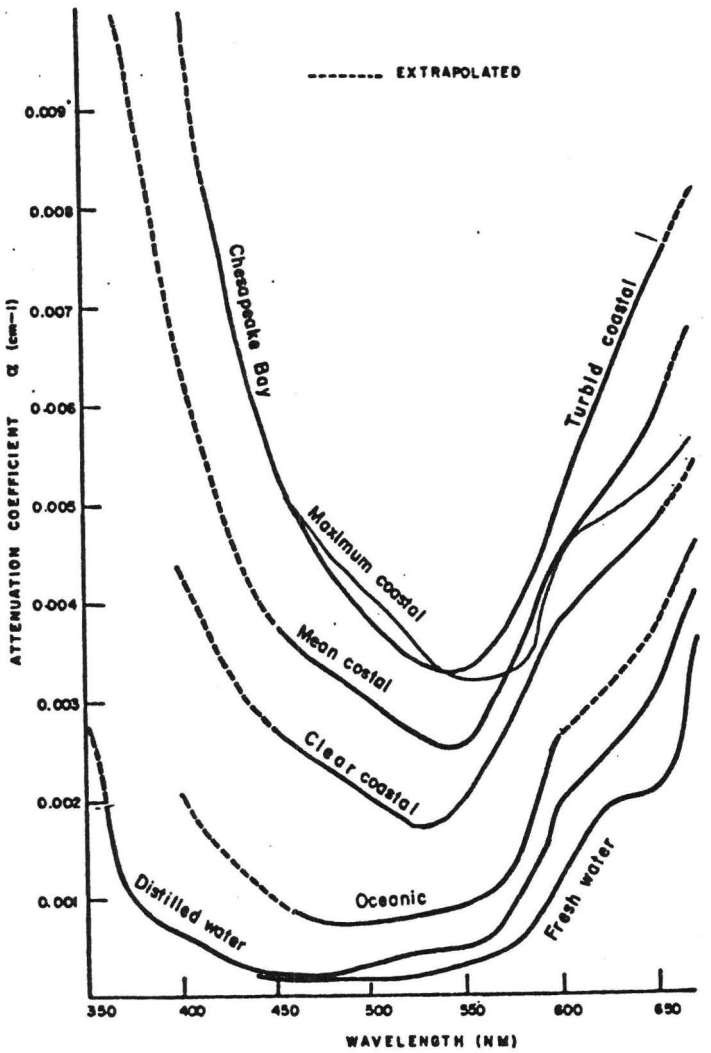

Figure 4. Attenuation coefficients of fresh water and sea water as a function of wavelength (modified from Polcyn and Rollin, 1969).

the attenuation of luminescence emitted at 589 nm from 1/2 m (metre) of water containing rhodamine WT dye ranges from 4% for distilled water to 18% for average coastal water. For comparison, tap water at Lakewood, Colorado, at 17° C shows a 13% attenuation. These considerations indicate that rather than observing a linear relationship between luminescence and depth of water containing rhodamine WT dye, a factor is introduced that is directly proportional to the attenuation. For example, the luminescence of rhodamine WT, as measured in 1/2 m of distilled water with an FLD, would be 48 times more intense than the same concentration of rhodamine WT measured in a centimetre quartz cell with a laboratory spectrometer. The luminescence would be 43 times more intense if Lakewood tap water were used as the solvent.

Accordingly, in the following discussion, which concerns quantifying the luminescence of crude and refined oils and plants in terms of rhodamine WT dye equivalency, the integrated rhodamine WT dye equivalent for the material is divided by 43 to allow for the difference in the depth of the dye column as viewed by the spectrometer and by the FLD.

The rhodamine WT equivalencies discussed below and shown on the graphic data should be considered reliable as predicted with corrections noted above. However, the actual field observation with an FLD may depart from these predicted values by as much as an order of magnitude due to varying atmospheric and seasonal conditions, temperature dependence of luminescence, time of day, and instrument sensitivity.

4. DESCRIPTION OF THE FRAUNHOFER LINE DISCRIMINATOR

Perkin-Elmer instrument

The redesigned Perkin-Elmer FLD (figure 5) consists of an optical head, electronic console, and light collector. The main components in the optical head are two telescopes, one earth-looking and one sky-looking; a rotating optical chopper wheel; three replaceable optical filter sets; and a photomultiplier with its power supply. Sunlight and skylight falling

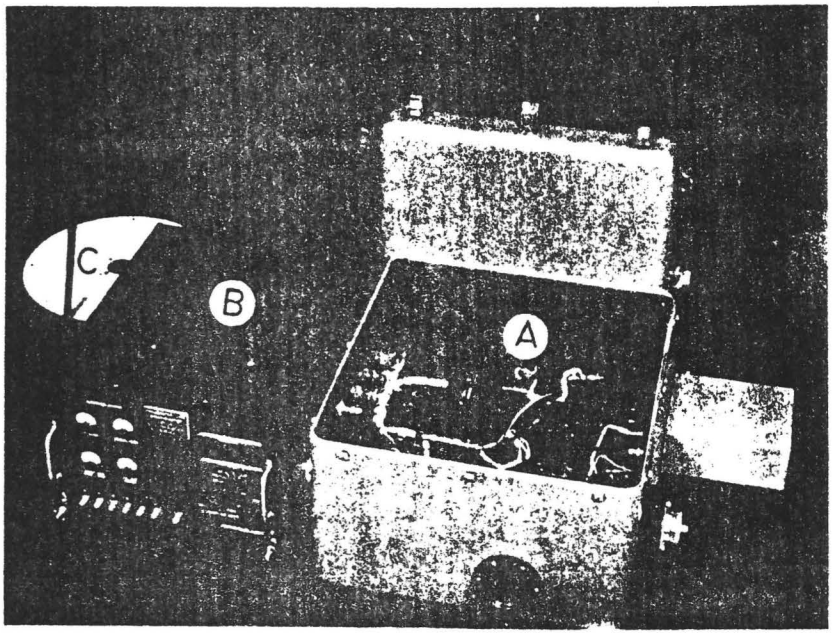

Figure 5. Perkin-Elmer redesigned FLD, showing the optical head (A), electronic console (B), and light collector (C).

on the diffuse surface of the light collector are reflected by a mirror into the sky-looking telescope. The earth-looking telescope observes the target whose reflectivity and luminescence are to be measured. Light from the two telescopes is sequentially routed through two different paths by the rotating chopper wheel. In one path, light passes through a filter which is centered at a specific Fraunhofer line but whose bandpass is several hundredths nanometres wider than the Fraunhofer line. This signal constitutes the light

intensity measured on the solar continuum adjacent to and including the Fraunhofer line, and is designated signal "a" in the sky-looking channel and signal "d" in the earth-looking channel. In the other path, a Fabry-Perot interference filter, with half-width of less than 0.07 nm, passes light coincident with the intensity of the central part of the Fraunhofer line; this signal is designated signal "b" in the sky-looking channel and signal "c" in the earth-looking channel. These signals are fed to a mini-computer that generates luminescence and reflectance by solving the following equations: $\rho = (d - c)/(a - b)$; $\varepsilon = (d/a) - \rho$, where ρ is reflectance and ε is the luminescence coefficient. Both ρ and ε are displayed as four-digit numbers (from 0000 to 9999 counts) on the front panel and are fed to a digital printer for permanent record; hence, 100 counts for ρ or ε implies a reflectance or luminescence of 1 percent. Reflectance values are displayed and recorded as percent directional reflectance. Inasmuch as displayed and recorded luminescence are only proportional to true luminescence for each substance measured, the luminescence count is referenced to the count from a standard (such as a dye sample or a photographer's gray card), permitting relative luminescence measurements to be made.* An automatic gain control (AGC) is used to monitor and maintain the a-signal at a nearly constant level by varying the gain of the photomultiplier tube (PMT detector). This permits measurements under a wide range of illumination and allows the PMT to operate at full gain under low illumination. Three sets of Fabry-Perot filters are available, permitting measurement at the 656.3-, 589.0-, and 486.1-nm Fraunhofer wavelengths. Additional filters can be fabricated at other Fraunhofer wavelengths, including 396.8, 422.7, and 518.4 nm.

Funding for the design and construction of the Perkin-Elmer engineering model FLD was provided by NASA's Advanced Application Flight Experiments (AAFE) Program.

*Reflectance and luminescence values are presented in this report in terms of their mean plus or minus the standard deviation of the mean (Hoel, 1965, p. 139).

Isomet instrument

The Isomet FLD consists of an optical head, electronics console, and light collector as shown in figure 6. The optical head consists of two telescopes, one earth- and one sky-looking; an electronic tuneable filter, and photomultiplier with power supply. Incoming radiation through each

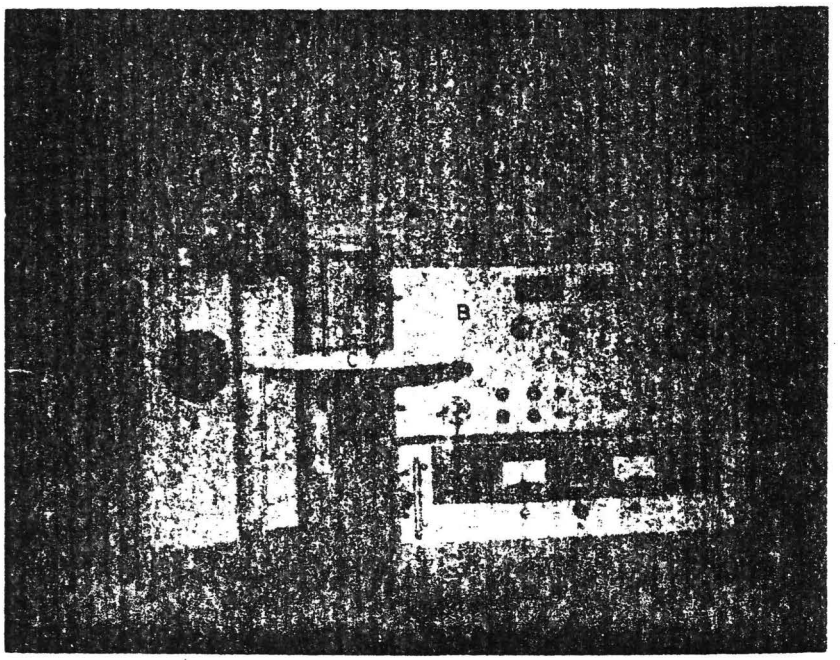

telescope is alternately viewed by a chopper and sequentially routed to a polarizing beam splitter, where it is linearly polarized, and then to the electronically tuneable filter (ETF). This is a solid state device which has the unique capability of changing its optical transmission with the frequency of an applied electrical signal. The ETF consists of a crystal into which an acoustical wave has been induced. This acoustical wave rotates the polarization of a very narrow spectral component of the incoming

radiation by 90°. All of the light incident on the ETF is retro-reflected by a mirror on one end of the crystal the beam emerges and is again incident upon the beam splitting polarizer. The unselected portion of the beam which is unaltered in polarization is directed back toward the source. The selected portion, having been rotated 90° is deflected by the polarizer and appears as the desired monochromatic light beam. The center wavelength of the optical bandpass is inversely proportional to the frequency of the electric signal and can be tuned throughout the visible spectrum. In order to achieve the required narrow bandwidth for the FLD, it was necessary to use the ETF's in tandum, thereby narrowing the wavelength resolution to less than 0.1 nm at the blue end of the spectrum to slightly greater than 0.1 nm at the red end. Transmission losses through the tandum ETF's proved to be greater than expected and this coupled with excessive photo-multiplier noise due to thermal emission, greatly reduced the sensitivity, especially at wavelengths less than 486.1 nm. Since several acoustical frequencies can be propagated simultaneously in the crystal, the ETF operates concurrently at several discrete wavelengths. "a", "b", "c", and "d" isgnals are simultaneously generated using this characteristic. These signals are fed to a mini-computer that calculates luminescence by solving the luminescence equation. Luminescence is displayed as a three digit number (from 000 to 999 counts) on the front panel and fed to a digital printer for permanent record. An automatic gain control is used as with the Perkin-Elmer FLD, with the exception that it can be by-passed and the photomultiplier voltage controlled manually.

Development of the FLD by Isomet Electronics was supported by NASA's Supporting Research and Technology (SR&T) Program.

Ground based measurements

Initial ground tests of the redesigned Perkin-Elmer Fraunhofer line discriminator were conducted outdoors at the Denver Federal Center, Lakewood, Colorado during the spring and summer of 1974. These tests were designed to determine the FLD operating characteristics with various sky conditions and with materials of various reflectance and luminescence properties.

The ground test configuration is shown in figure 7. The optical unit was mounted on a moveable platform under which various targets, including a tank filled with water to a depth of one-half metre, can be positioned and illuminated by the sun without shadows from the supporting structure. A dual channel digital recorder simultaneously recorded luminescence and reflectance. Measurements were made on a variety of natural materials (results described in section 6.0) and on selected luminescence and reflectance standards. The rhodamine WT equivalent luminescence of each standard as measured with the FLD was confirmed with a laboratory fluorescence spectrometer using procedures described in section 3.0. Measurements on selected luminescence standards are shown in the following Table (equivalent rhodamine WT concentration in ppb; source, detector, solar, and depth corrected).

Table 1. Comparison of luminescence of selected standards measured with the laboratory fluorescence spectrometer and the FLD at specific Fraunhofer lines.

Material	Luminescence (spectrometer)			Luminescence (FLD)		
	486.1 nm	589.0 nm	656.3 nm	486.1 nm	589.0 nm	656.3 nm
Blue paint	4.6			3.3		
Green paint		.9			1.9	
Red paint		13.0			22.0	
Fluorescent cloth		133.0	115.0		109.0	102.3

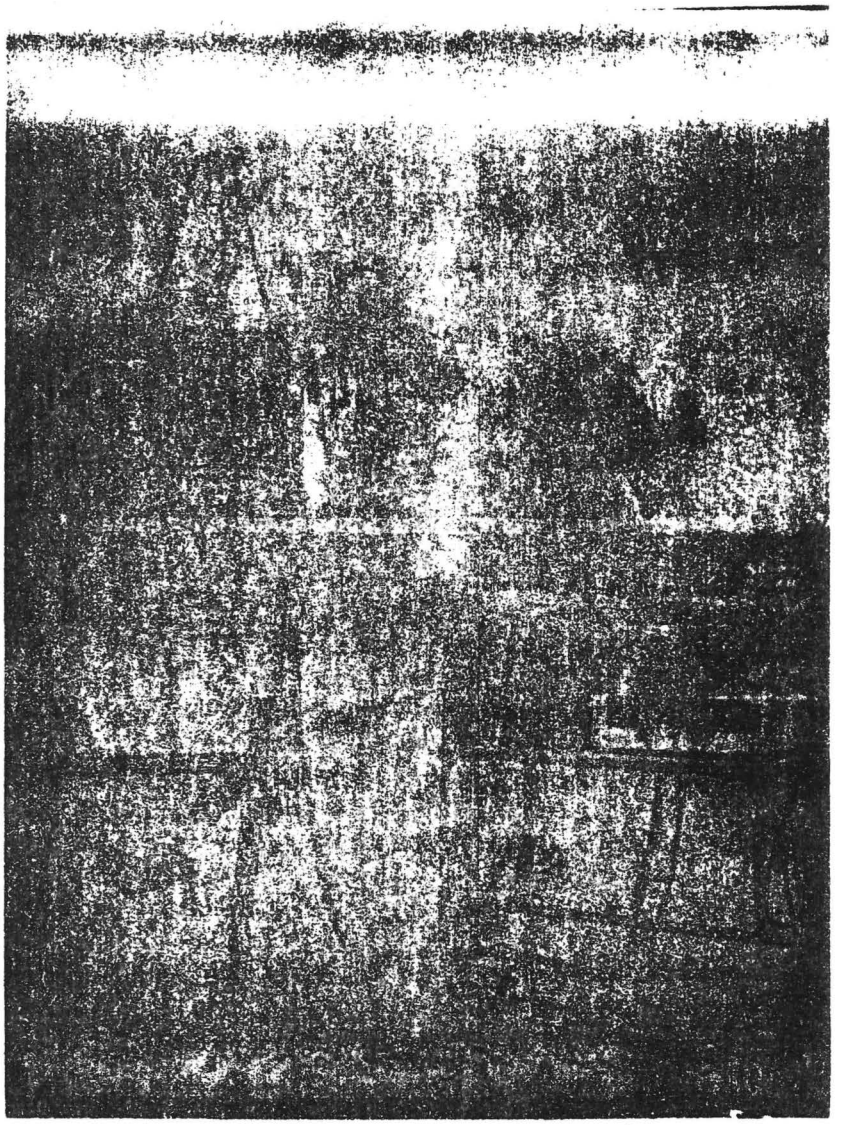

Figure 7. FLD ground test configuration showing pyrex tank containing water 1/2 metre deep beneath optical head.

Ground tests show that rhodamine WT dye can be detected at the 589.0 nm Fraunhofer line in one-half metre of water under clear sky conditions in concentrations as low as 0.1 ppb; however, sensitivity under field conditions is generally considered to be 0.25 ppb. The relationship between dye concentration and luminescence measured by the instrument is approximately linear, with 1.3 ppb per 100 FLD counts at the 589.0 nm line under clear sky conditions. An operational characteristic that adversely affected the performance of the FLD during the initial tests was the strong dependence of luminescence on reflectance, particularly under cloudy conditions. Typically a change in reflectance of 80% would cause a change of 100 counts (clear sky) and 300 counts (cloudy sky) in luminescence, and introduced an "apparent" luminescence of a highly reflective material of some 300 counts, or up to 3.9 ppb rhodamine WT equivalent, a greater magnitude of luminescence than most of the natural materials being measured. This problem arose because of the critical nature of the optical balance of the Perkin-Elmer FLD; however, a solution which significantly reduced the reflectance dependence to less than $\pm$ 10 counts for an 80 percent reflectance change is described in section 7.0. Measurements under both clear and cloudy conditions demonstrate that the sensitivity of the FLD under clear skies is greater than under clouds. For example, comparison of ground measurements on gray card standards consistently showed 25 percent higher luminescence for clear sky versus cloudy conditions; similar results were achieved in airborne measurements of phosphate rock and gypsum in Florida where differences in luminescence under cloudy and clear conditions ranged from 23 to 38 percent.

In addition to the tests on the Perkin-Elmer FLD mentioned above, the sensitivity of the Isomet FLD was compared to the Perkin-Elmer FLD at the

656.3 nm Fraunhofer wavelength. The two units were operated concurrently outdoors at the Denver Federal Center. Fluorescent red cloth was selected as a standard because it was available in a size appropriate as a ground calibration target for airborne operations. When viewing this material, the Perkin-Elmer and Isomet FLD's read luminescence counts of 2750 and 1750 counts, respectively. The Isomet FLD required twice the warm up period (45 minutes) of that of the Perkin-Elmer FLD (20 minutes), but sensitivity deteriorated markedly for the Isomet instrument following the warm-up period. Sensitivity, measured in terms of the minimum concentration of rhodamine WT detectable in one-half metre of water at 20° C., is 0.25 ppb for the Perkin-Elmer instrument. Sensitivity for the Isomet instrument is 1.0 ppb measured during the period of optimum performance at the end of the 45 minute warm-up period.

An attempt to measure sulfite liquor and phosphate rock at 486.1 nm was not successful with the Isomet FLD, although these materials were readily detectable with the Perkin-Elmer FLD.

Airborne measurements

The Fraunhofer line discriminator was first operated as an airborne fluorometer aboard a Bell Jet Ranger helicopter at Lake Michigan, near Pentwater, Michigan (see section 6.0). Figure 8 shows the FLD optical head and light collector installed in a basket located near the middle of the fuselage. During trial mounting, the optical head was mounted high,

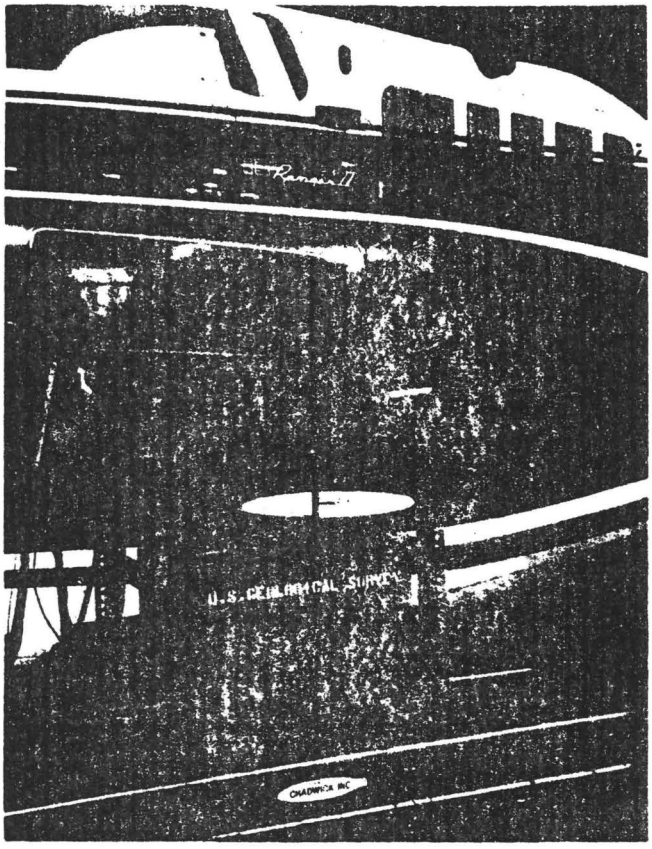

Figure 8. FLD optical head and light collector installed in a basket mid-ship on a Bell Jet Ranger helicopter.

close to the rotor blades to avoid reflections from the sides of the fuselage, but this caused considerable degradation in the FLD performance, probably due in part to synchronization of rotor blades with a harmonic of the instrument bandwidth. The lower mount proved satisfactory and has

been used in all succeeding helicopter experiments. The most consistent results were achieved when the diffuse surface of the light collector had approximately the same orientation to the sun during a series of traverses, and when shadows of the tripod legs did not obscure the aperature of the sky-looking telescope.

Figure 9 shows the installation of a tray containing black, gray, and white cards, and rhodamine WT for reflectance and luminescence standards.

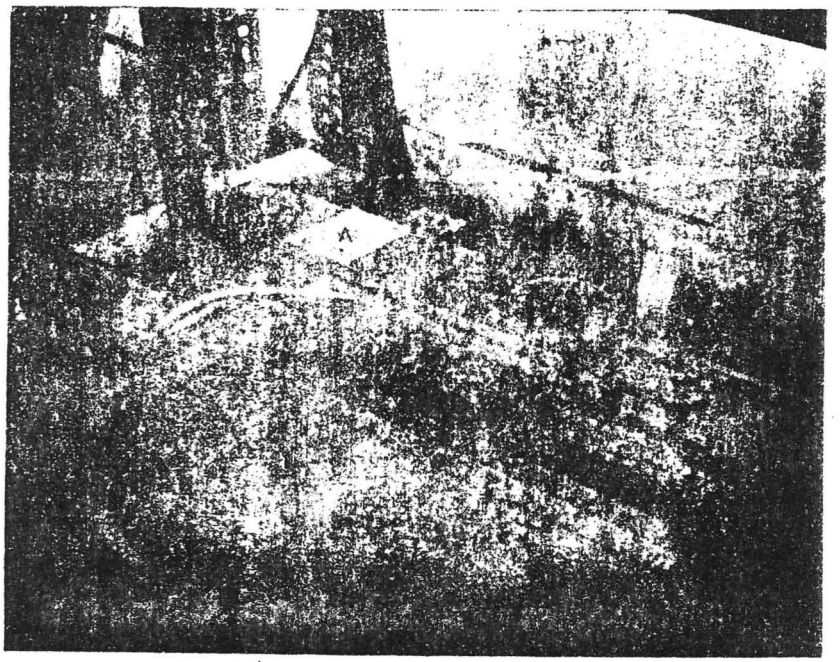

Figure 9. Calibration tray containing white, gray, and black reflectance standards (A,B, and C, respectively) and a rhodamine WT standard, D.

The tray was mounted below the earth-looking telescope and was brought into the field of view by a motor driven rack for inflight calibration. Although the calibration tray worked satisfactorily, subsequent experiments have used a single luminescent cloth panel deployed on the ground for an inflight systems check, and several reflectant and luminescent chips, 20 x 25 centimetre (cm), which were place beneath the ground-looking telescope for pre- and post-flight calibration.

The work at Lake Michigan showed that sun glint is to be avoided over water targets because intermittently high and low reflectance values occur in these areas, apparently at a higher frequency than can be tolerated by the FLD computer. Visual identification of the water areas being observed with the FLD and location of marker buoys in the FLD field of view was also very difficult. Following the Lake Michigan experiments, therefore, a viewing system was developed and field tested which includes: 1) a television camera with a remotely controlled focus and zoom lens for monitoring the target measured with the FLD, 2) a second television camera which monitors a bank of light emitting diodes containing reflectance and luminescence data that are continually updated by the digital output of the FLD, 3) a tape recording system for recording the data from both cameras and voice description, and 4) a television monitor on which is displayed a real time the target scene upon which is superimposed the reflectance and luminescence counts. Boresighting of the viewing system is achieved by positioning a luminescence panel on the ground and marking the position of the panel on the television screen by the luminescence indicated while hovering over the panel. The viewing system has proven dependable and allows discrimination of small luminescence targets which would otherwise be lost in data reduction. It also permits storage of the data in a form which can be recovered rapidly.

Current operational procedures for airborne measurements with the FLD are as follows:

1. Optical filter and electronic warm-up -- 30 minutes for the Perkin-Elmer instrument and 45 minutes to one hour for the Isomet instrument. Because reserve electrical power of most helicopters is limited, a DC inverter operating from a 12-volt automobile battery is used for on-the-ground standby power.
2. Pre-flight calibration using reflectant and luminescent chips.
3. In-flight systems check using a ground-deployed luminescent panel.
4. Airborne luminescence and reflectance measurements over target area.
5. Post-flight calibration using reflectant and luminescent chips.

Air temperature, extent of cloud cover, and other meteorological parameters, as appropriate, are recorded throughout the day.

Luminescent dyes

Rhodamine WT, rhodamine 6GDN, rhodamine B, and uranine B are water soluble luminescent dyes used by marine geologists and hydrologists to monitor current dynamics in rivers, estuaries, and coastal waters. Conventional methods of monitoring dispersal and transport of the dye are awkward. One method involves boat traverses of the dye cloud and the collection of water samples which are subsequently analyzed for dye concentration with a laboratory fluorometer. A disadvantage of this approach is that the boat disrupts the normal dispersal of the cloud. Another method is to photograph the dye cloud from an aircraft, but this approach is satisfactory only when dye concentrations are relatively high, and when lighting conditions permit marked contrast between light reflected from the dye cloud and from the uncontaminated water. Neither method permits immediate availability of the data.

The FLD has the sensitivity to detect rhodamine WT dye in 1/2 m of water in concentrations of 0.25 ppb or less at 20° C. During the week of June 9, 1974, a joint U.S. Geological Survey--U.S. Army Coastal Engineering (CERC) experiment was conducted at Charles Mears State Park, Pentwater, Michigan, using the dyes noted above as tracers to study currents along the shore of Lake Michigan. The experiment was conducted to determine the feasibility of detecting the mapping luminescent dyes with the airborne redesigned FLD and making the traverse results immdiately available in the field.

Prior to the Lake Michigan experiment, the luminescence of selected dyes (rhodamine 6GDN, uranine B, and rhodamine B) supplied by CERC were measured in the laboratory using a laboratory fluorescence spectrometer. These measurements show that the 589 nm Fraunhofer line is optimum for the Pentwater experiment because all the dyes show relatively high luminescence intensities at this wavelength.

The FLD was flown on a Bell 206 Jet Ranger helicopter. The selected flight altitude was approximately 75 m (250 ft.) above the lake at a speed of 16-32 km/hr (10 to 20 miles/hr) indicated air speed. The results of June 13 are shown in Figure 10. The dyes were placed at fixed locations at distances of 152, 229, and 304 metres (500, 750, and 1000 ft.) from shore and released into the water at nearly the same time (within three minutes).

Several runs both perpendicular and diagonal to the direction of dye flow were made, with the time of each run shown in Figure 10. The diagonals were selected to increase the number of measurements near the points of release and were flown in a southwest direction. The numbers along each run are the average of 10 luminescence counts, and the distance between each number represents a distance of approximately 22 m (75 ft.). The total distance of each run varies from approximately 213 to 304 m (700 to 1000 ft.). Based on the average counts, isopleths representing equal luminescence intensity have been drawn for the rhodamine 6GDN, rhodamine B, and uranine B dye clouds; the isopleth interval varies from 15 to 200 counts. FLD readings shoreward from the uranine B and rhodamine B clouds range from 8 to 49; these are the residue of an earlier dye release, and isopleths were not drawn in this area.

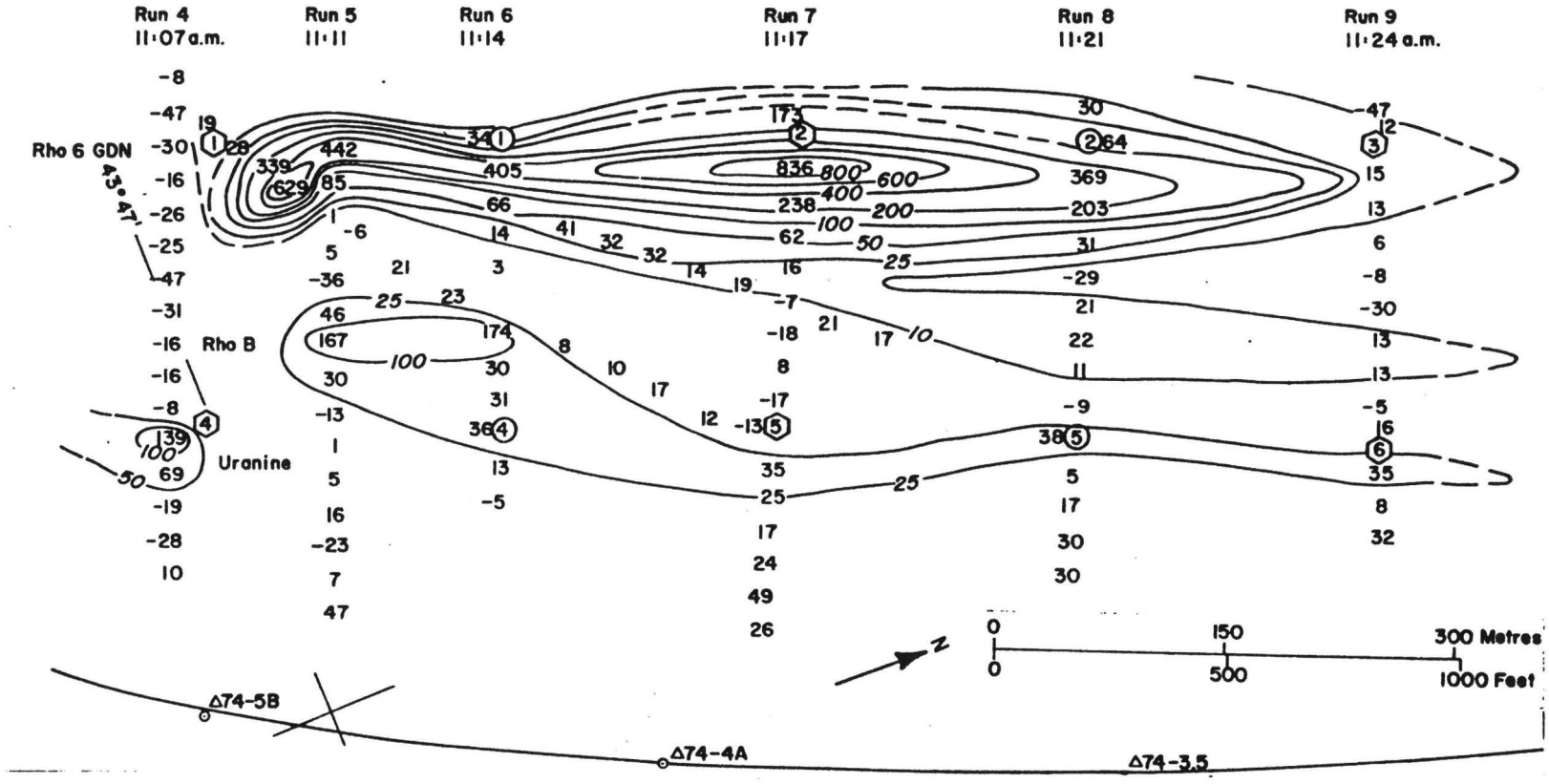

CHARLES MEARS STATE PARK

Figure 10. Dye concentration patterns based on unreduced FLD readings made on eight runs during late morning (11:07-11:34), June 13, 1974. The three dyes were released at points 152, 229, and 304 m (500, 750, and 1000 ft.) from shore between 10:26 and 10:28 a.m. Numbered circles and triangles are anchored buoys and on-shore reference points.

Calibration curves in figure 11 show FLD luminescence counts plotted as a function of dye concentration in parts per billion. These curves

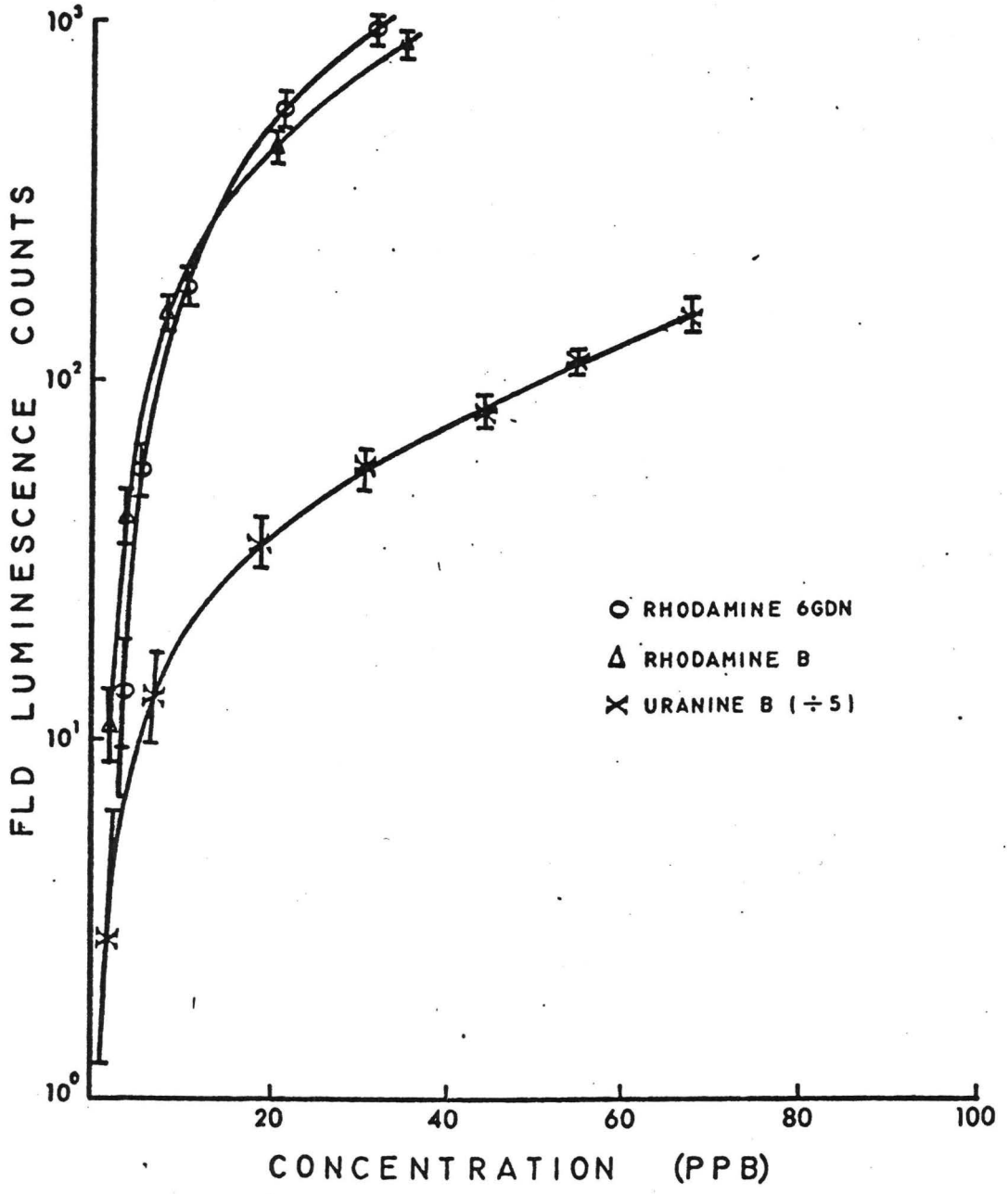

Figure 11. Luminescence versus dye concentration obtained during calibration of the FLD. The three curves were obtained by varying the concentration of each dye separately in a tank containing 0.5 m of water. Luminescence counts were measured with the FLD suspended above the tank. Note that the abscissa has been reduced by a factor of 5.0 for uranine B.

were obtained with the FLD by measuring the luminescence of each of three dyes separately at a known concentration in a tank of water. The FLD was suspended over the tank and the mean and standard deviation of luminescence counts measured for each concentration. These curves permit conversion of the luminescence FLD counts shown in figure 11 into dye concentration in parts per billion (ppb).

The Pentwater, Michigan test was the first opportunity for aircraft operation of the new FLD; probably the most significant result of this test was the experience in operational methodology and general "shake-down" of the instrument and field procedure. It is believed that temporal dispersion of dye plumes can be monitored, areally quantified, and mapped from a helicopter with the FLD.

Geochemically stressed vegetation

The relationship between luminescence and photosynthesis in plants is complex, but in general, factors that both impede and enhance photosynthesis can modify luminescence (Hollaender, 1956). Several such factors exist in nature. Based on the air pollution work of O'Gara (1922), Thomas (1961, p. 236-237) ranked cultivated and native plants according to resistance to sulfur dioxide fumigation. Although luminescence effects were not studied, Thomas noted substantial variability in sulfur dioxide susceptibility of some species, including conifers, but others were relatively constant. Alfalfa, barley, and cotton were most sensitive. Using alfalfa as unity, elm, birch, sumac, and poplar were about 2.5 times more resistant, pine 7-15 times more resistant, and live oak 12 times more resistant. Thomas (1961, p. 253) also noted that 3-4 month old ponderosa needles were sensitive to hydrogen fluoride fumigation, but that old needles were resistant. Another such factor is geochemical stress, where toxic concentrations of one or more metallic elements may subject plants to chemical and physiological changes. Copper and zinc are toxic if present in large quantities (Kramer and Kowlowski, 1960, p. 225-226) and are reported to produce symptoms closely resembling iron chlorosis (Sauchelli, 1969, p. 65). J. E. McMurtrey (in Sauchelli, 1969, p. 156) notes that copper in excess of 0.1 ppm stunted tobacco plants. F. A. Gilbert (in Sauchelli, 1969, p. 158) states that growth of tomatoes in nutrient solution was reduced by as little as 1 ppm copper. Sauchelli (1969, p. 112) cites zinc having a toxic effect in some cereal grains where levels exceed 150 ppm, and in citrus where levels exceed 220 ppm. K.C. Beeson (in Sauchelli, 1969, p. 133 and 138) reports that concentrations of molybdenum in plants may vary from less than 0.1 ppm to more than 300 ppm without adverse effect on growth. Press (1964, p. 374-375)

reports that bean plants grown in solutions containing varying concentations of lead exhibited chlorosis and that spectral reflectance at 550 nm ranged from 15 percent for 1 part per million (ppm) lead to more than 30 percent

Watson, Hemphill, and Hessin (1973) grew bean plants hydroponically and treated them with varying metal concentrations, including molybdenum, copper, zinc, and lead, to demonstrate that luminescence is an indicator of geochemical stress produced by metal toxicity. Measurements were made both in the early stage of growth and at full maturity. Table 2 shows luminescence differences observed for 10 plants, five nonstressed and five stressed with 10 ppm sodium molybdate ($NaMO_4$). Both groups were grown in a Hoagland #2 solution.

Table 2. Luminescence (source-detector, solar and depth corrected) of 10 bean plants expressed in terms of rhodamine WT equivalency (ppb). The plants were grown hydroponically in Hoagland #2 nutrient solution; five of these plants were geochemically stressed with 10 ppm sodium molybdate ($NaMO_4$).

	Stressed		Nonstressed	
Description	2 weeks	5 weeks	2 weeks	5 weeks
Top surface, large trifoliate leaves	0.62	1.05	0.45	1.19
Top surface, small trifoliate leaves	0.67	0.64	0.49	0.98

Differences in luminescence at two weeks are reversed at five weeks. The reversal not only occurs between stressed and nonstressed plants but also between large and small leaves. The difference in luminescence is reduced at five weeks for the large leaves. These results illustrate the complexity of luminescence during various stages of growth, and tend to support the

observations of Thomas (1961) in his plant fumigation experiments noted above.

To investigate the luminescence of needles of Pinus ponderosa, trees growing in a copper- and zinc- rich soil near Malachite Mine, Jefferson County, Colorado (Figure 12) were measured in the field using the laboratory fluorescence spectrometer and were compared to measurements of needles from background trees. Country rock where trees grow includes biotite schist and hornblend gneiss, and younger pegmatite dikes; all are of Precambrian age (Huff, 1963).

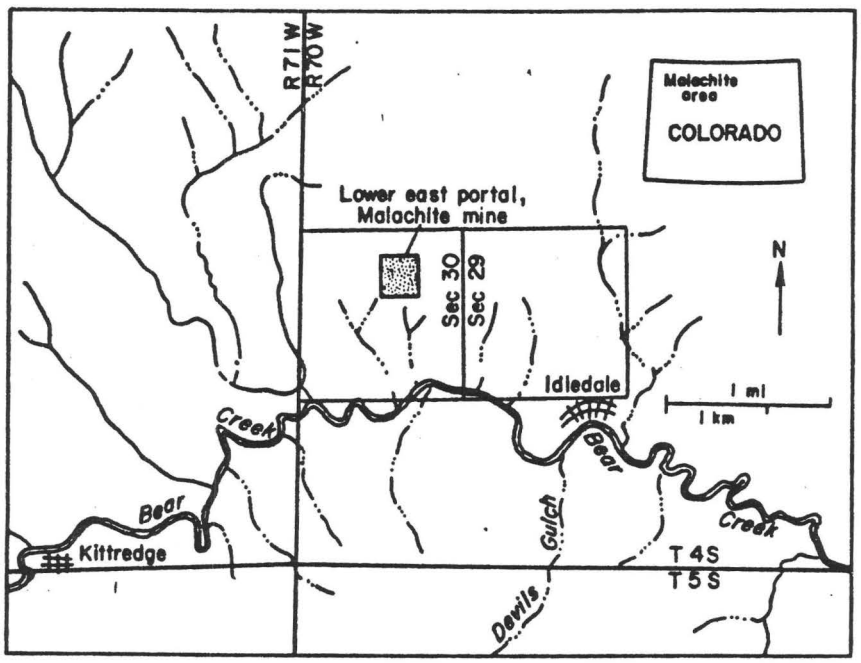

Figure 12. Location of Malachite Mine area, Jefferson County, Colorado. Stipple pattern shows area of Figure 13. Modified from Huff (1963).

Figure 13 shows the copper anomaly in the Malachite Mine area, and the location of background and geochemically stressed tree groups. Measurements

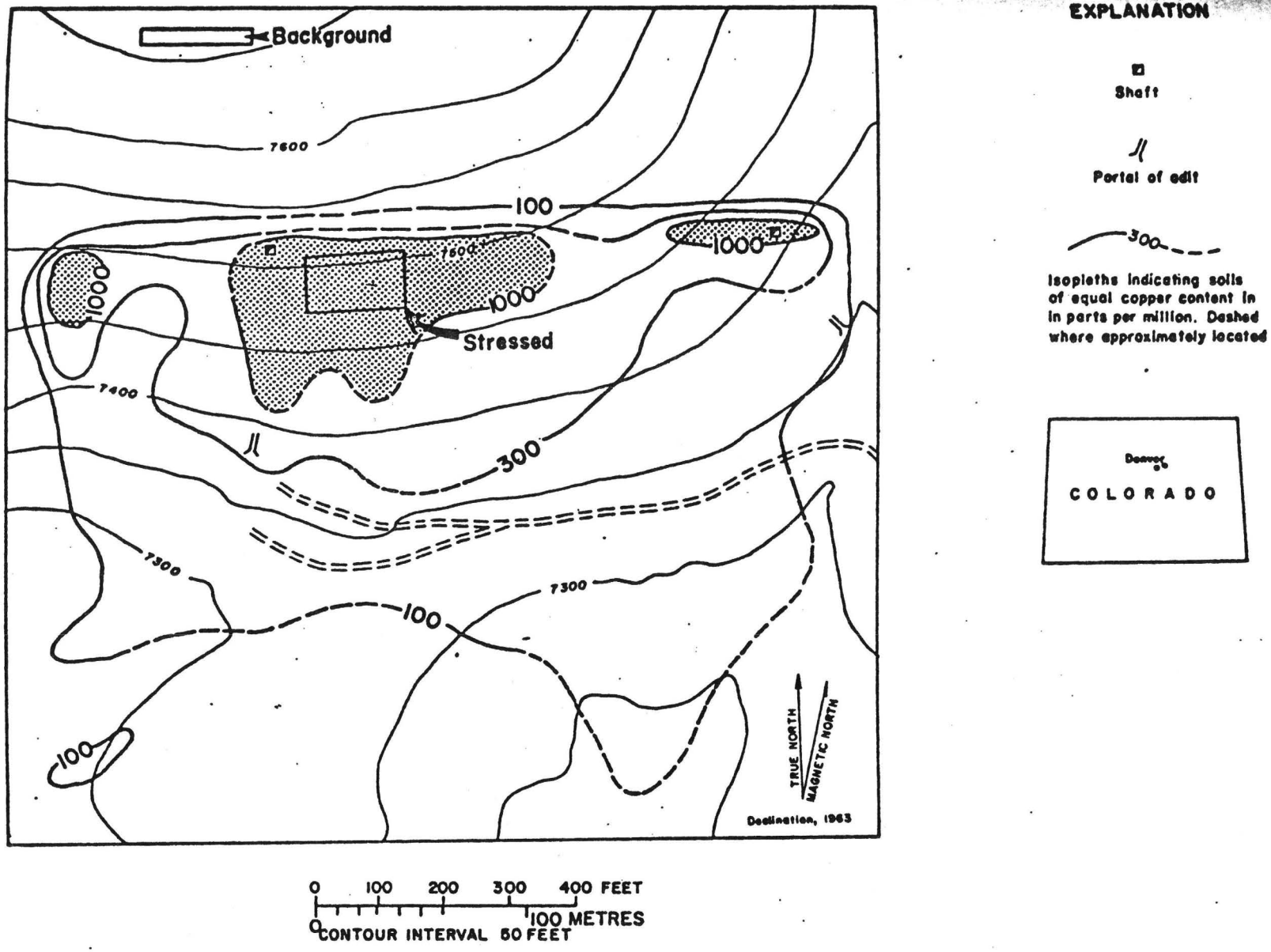

Figure 13. Distribution of copper and location of sample trees growing in background and anomalous soils (modified from Huff (1963).

were made both diurnally (every four hours over a 24-hour period) and seasonally (every 4-5 weeks, July-November 1973 and April-May 1974). Data during the period from December 1973 through March 1974 could not be obtained because of heavy snow. Four twigs were collected from each of seven background and geochemically stressed trees making a total of 56 samples that were measured. The needles were removed from the twigs, placed on a black-matt nonluminescent surface, and measured in the front-surface mode in the spectrometer. The four-hour spacing between separate collection runs was determined by the time required for sample collection, measurements, and logistical considerations, but it was verified that the period of as much as two hours between time of collection and completion of measurement did not alter the luminescence of the needles beyond experimental error.

Subsequent measurement of copper and zinc in the ash of the needles was determined by standard analytical techniques, and Table 3 shows the results of chemical analyses of samples collected during late summer and autumn of 1973. Mean copper content of ash from stressed trees on four dates exceeds

Table 3. Mean and standard deviation of the mean of copper and zinc content (parts per million) of needle ash from 13 Pinus ponderosa growing in geochemically anomalous and background soils.

Sample Date	Anomalous Trees		Background Trees	
	Copper	Zinc	Copper	Zinc
July 26, 1973	175 ± 16	>2000	110 ± 7	730 ± 25
August 30, 1973	180 ± 8	2180 ± 77	115 ± 4	1130 ± 30
Oct. 18, 1973	125 ± 5	2330 ± 36	100 ± 7	700 ± 84
Nov. 12, 1973	140 ± 7	2080 ± 35	100 ± 4	880 ± 30

the mean copper content of the background tree ash by factors of 1.2 to 1.6. Mean zinc content of stressed tree ash exceeds the background trees by factors of 1.9 to 3.3.

Distribution of copper in the soil in the vicinity of the Mine is given by Huff (1963). Additional ash analyses for copper content of 16 trees in the area are given by Howard, Watson and Hessin (1971).

Figure 14 shows the spectral excitation curves obtained in March 1973 for both groups of trees and also for rhodamine WT dye at a concentration of 1200 ppb. The integrated excitation intensity is significantly greater for background than for stressed trees; solar-corrected rhodamine WT equivalency are 19 ppb and 5 ppb, respectively. Solar- and depth-corrected rhodamine WT equivalency are 0.4 and 0.2 ppb, respectively (see Section 3).

In order to test the sensitivity of the redesigned FLD to chlorophyll luminescence of stressed and nonstressed Pinus ponderosa, twigs were collected from seven stressed and seven background trees at the Malachite Mine site in early March 1974. Luminescence measurements were made within two hours outdoors at the Denver Federal Center. Figures 15 and 16 show that the difference between the mean luminescence of stressed and background trees is about 16 percent.

Following this initial experiment, the FLD was used from a helicopter to measure the luminescence of stressed and nonstressed Pinus ponderosa trees at the Malachite Mine, both on a diurnal and seasonal basis for the period of September 1974 through July 1975.

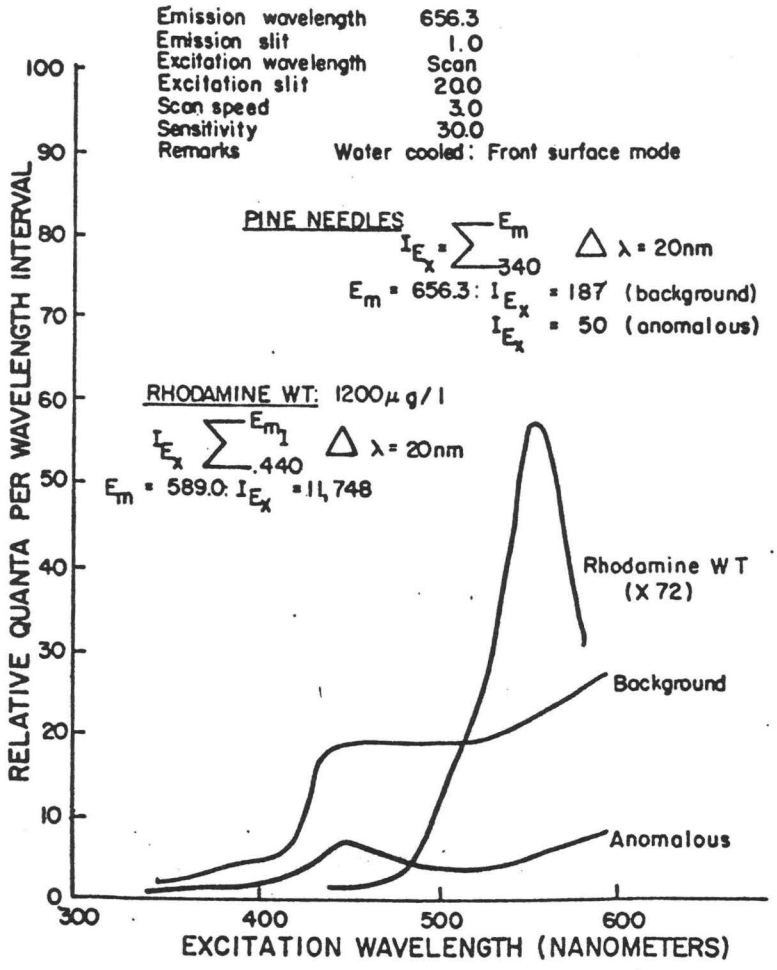

Figure 14. Excitation spectra of Pinus ponderosa needles from geochemically anomalous and background areas, Malachite Mine, Jefferson County, Colorado, as measured with a laboratory fluorescence spectrometer (source-detector corrected only). Integration of the area under each excitation spectrum permits comparison with the excitation spectra of a rhodamine WT standard.

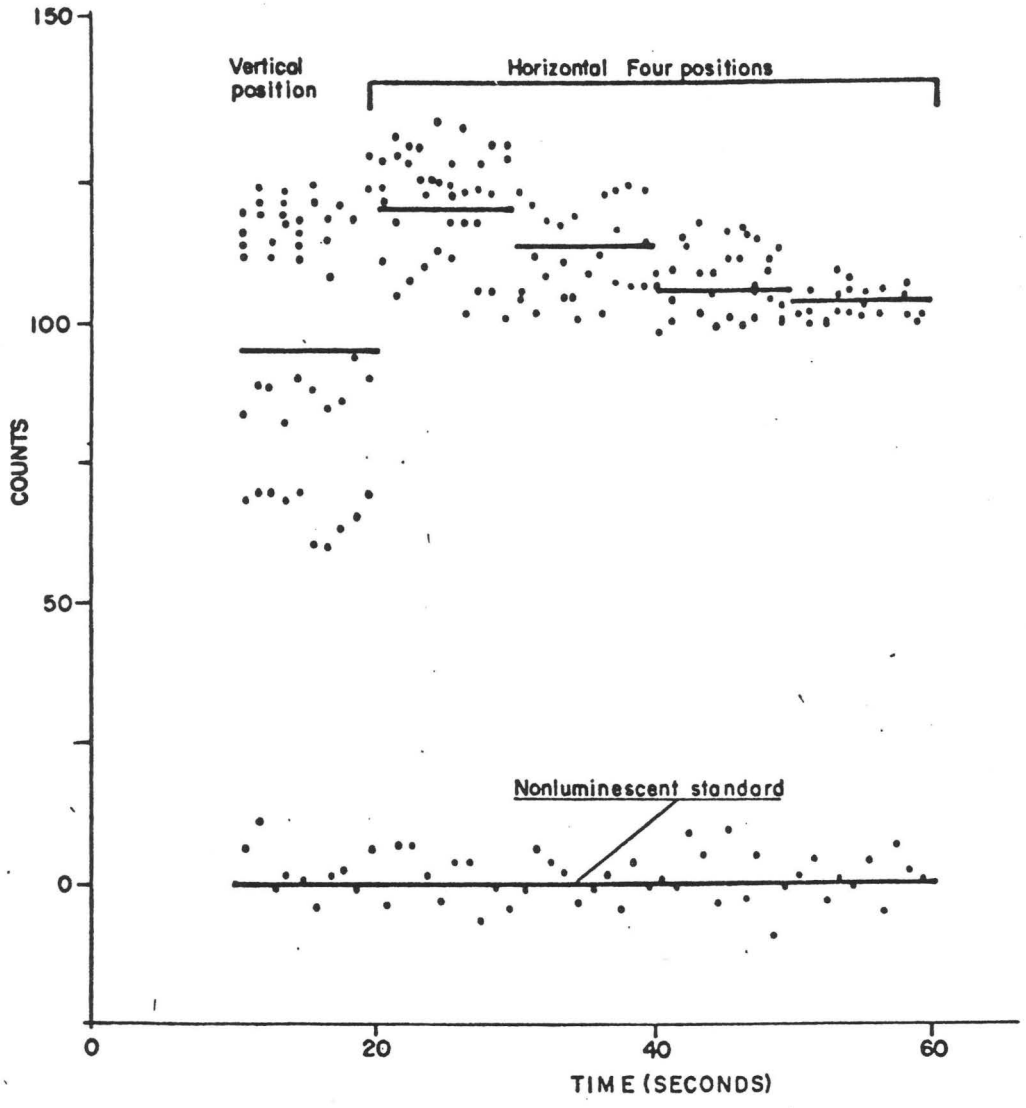

Figure 15. Relative luminescence of twigs averaged from seven trees growing in a geochemically background area, Malachite Mine, Jefferson County, Colorado. Mean and standard deviation of relative luminescence, 107.2 $\pm$ 1.0 counts, are measured in reference to nonluminescent gray-card standard (18 percent reflectance).

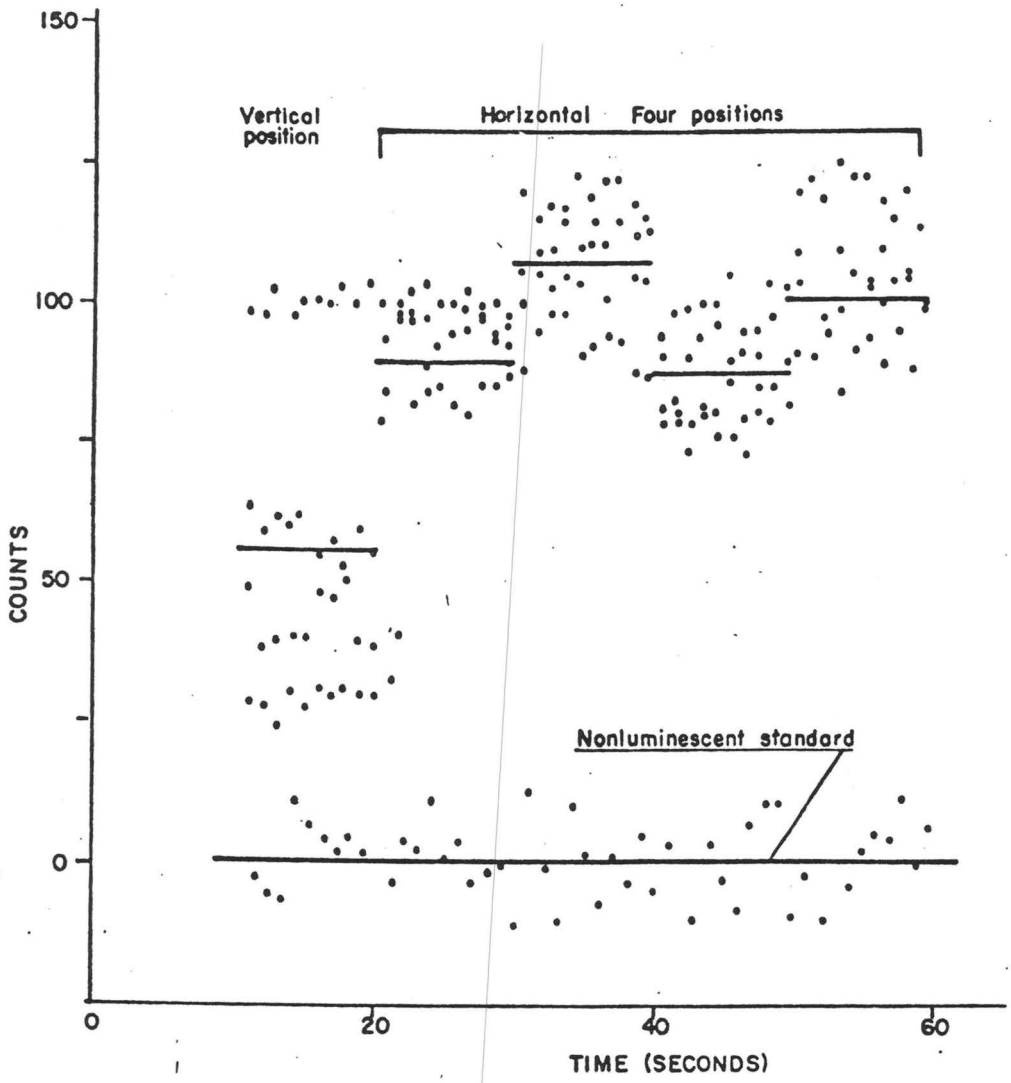

Figure 16. Relative luminescence of twigs averaged from seven trees growing in a geochemically anomalous area, Malachite Mine, Jefferson County, Colorado. Mean and standard deviation of relative luminescence, 90 ± 2.0 counts, are measured in reference to nonluminescent gray-card standard (18 percent reflectance).

These results combined with the results acquired with the fluorescence spectrometer during summer and autumn, 1973 and spring 1974 indicate that luminescence contrast between background and stressed trees was independent of air temperature, relative humidity, and wind speed, but maximum contrast, ranging from 1.6 to 2.2, tends to occur during parts of six days when cloud cover was less than 10 percent (Fig. 17)[1/]. On six days when cloud cover exceeded 10 percent, the diurnal luminescence trace of both groups tended to be similar and contrast did not exceed 1.4 (Fig. 18)[1/]. Data collected on September 28, 1973, September 24, 1974, and April 22, 1975 are exceptions (Fig. 19[1/]. A maximum contrast of 2.7 at 11:45 a.m. on September 28, 1973 was obtained during a period of 100 percent cloud cover. Contrast on April 22, 1975 does not exceed 1.4 despite cloud cover of less than 20 percent prior to 2 p.m. Contrast of 1.3 at 3:30 on September 24, 1974 is during a period of no cloud cover. An explanation for these exceptions is not known, although wind speed is somewhat higher for the three days shown in figure 19 than for the 12 days shown in figures 17 and 18.

Standard deviation of the mean for FLD ground measurements of twig samples from Pinus ponderosa at the Denver Federal Center in March, 1974 (see above), as well as for the fluorescence spectrometer measurements of trees during 1973 and 1974 at the Malachite Mine site ranged from less than one percent to three percent of the mean. However, standard duration of the mean of airborne FLD measurements during 1974 and 1975 frequently somewhat higher. This was due to the relatively sparse foliage of the Pinus ponderosa (which permitted bare ground to be observed through the foliage at relatively high frequency), whereas pine needles completely filled the field of view in both the spectrometer and ground based FLD measurements. This experience suggests that a smaller standard deviation may be assured in airborne measurements by avoiding species or individual trees with sparse foliage.

[1/] Standard National Weather Service nomenclature: relative humidity in percent, wind speed in miles per hour, and cloud cover in percent.

Figure 17. Temporal luminescence of Pinus ponderosa and meteorological parameters. Maximum luminescence contrast between background and stressed trees tends to occur during periods of minimum cloud cover.

Figure 18. Temporal luminescence of Pinus ponderosa and meteorological parameters. Minimum luminescence contrast between background and stressed trees tends to occur during periods of maximum cloud cover.

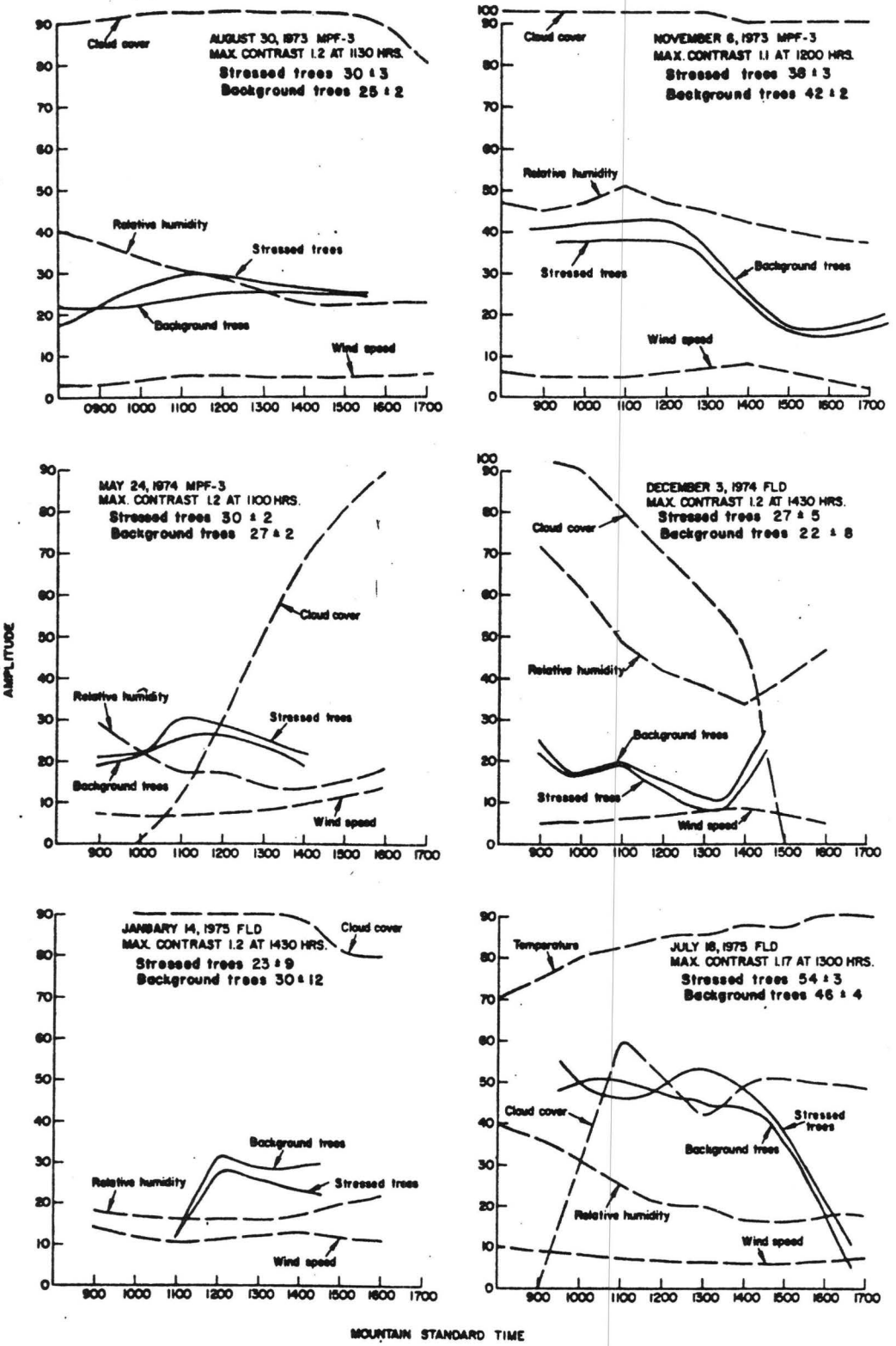
AUGUST 30, 1973 MPF-3
MAX. CONTRAST 1.2 AT 1130 HRS.
Stressed trees 30 ± 3
Background trees 25 ± 2
Cloud cover
Relative humidity
Stressed trees
Background trees
Wind speed
NOVEMBER 6, 1973 MPF-3
MAX. CONTRAST 1.1 AT 1200 HRS.
Stressed trees 38 ± 3
Background trees 42 ± 2
MAY 24, 1974 MPF-3
MAX. CONTRAST 1.2 AT 1100 HRS.
Stressed trees 30 ± 2
Background trees 27 ± 2
DECEMBER 3, 1974 FLD
MAX. CONTRAST 1.2 AT 1430 HRS.
Stressed trees 27 ± 5
Background trees 22 ± 8
JANUARY 14, 1975 FLD
MAX. CONTRAST 1.2 AT 1430 HRS.
Stressed trees 23 ± 9
Background trees 30 ± 12
JULY 18, 1975 FLD
MAX. CONTRAST 1.17 AT 1300 HRS.
Stressed trees 54 ± 3
Background trees 46 ± 4
Temperature
AMPLITUDE
MOUNTAIN STANDARD TIME

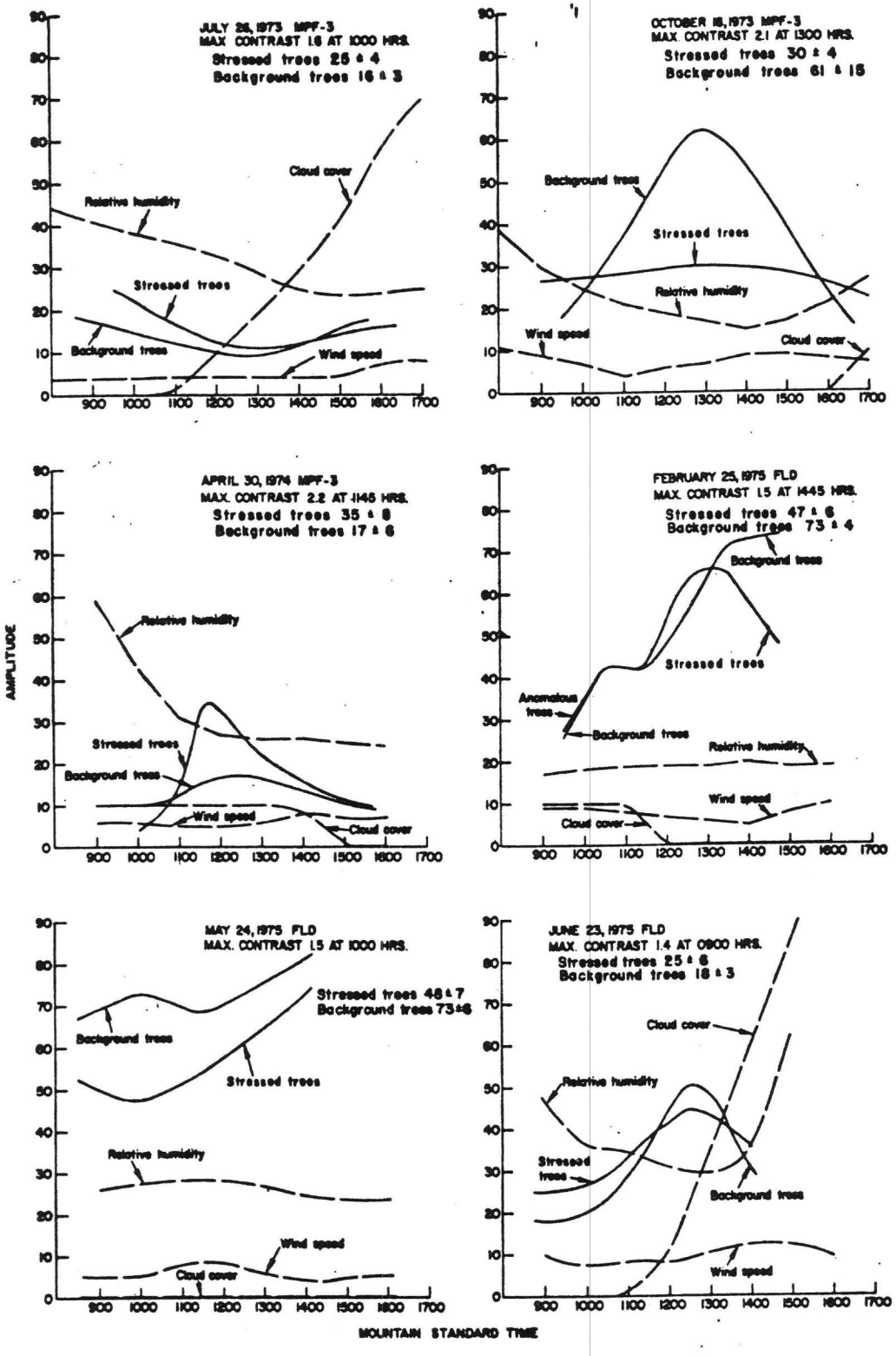
JULY 26, 1973 MPF-3
MAX. CONTRAST 1.6 AT 1000 HRS.
Stressed trees 25 ± 4
Background trees 16 ± 3
Cloud cover
Relative humidity
Stressed trees
Background trees
Wind speed
OCTOBER 18, 1973 MPF-3
MAX. CONTRAST 2.1 AT 1300 HRS.
Stressed trees 30 ± 4
Background trees 61 ± 15
Background trees
Stressed trees
Relative humidity
Wind speed
Cloud cover
APRIL 30, 1974 MPF-3
MAX. CONTRAST 2.2 AT 1145 HRS.
Stressed trees 35 ± 8
Background trees 17 ± 6
Relative humidity
Stressed trees
Background trees
Wind speed
Cloud cover
FEBRUARY 25, 1975 FLD
MAX. CONTRAST 1.5 AT 1445 HRS.
Stressed trees 47 ± 6
Background trees 73 ± 4
Background trees
Stressed trees
Anomalous trees
Background trees
Relative humidity
Wind speed
Cloud cover
MAY 24, 1975 FLD
MAX. CONTRAST 1.5 AT 1000 HRS.
Stressed trees 48 ± 7
Background trees 73 ± 6
Background trees
Stressed trees
Relative humidity
Wind speed
Cloud cover
JUNE 23, 1975 FLD
MAX. CONTRAST 1.4 AT 0900 HRS.
Stressed trees 25 ± 6
Background trees 18 ± 3
Cloud cover
Relative humidity
Stressed trees
Background trees
Wind speed
AMPLITUDE
0 10 20 30 40 50 60 70 80 90
900 1000 1100 1200 1300 1400 1500 1600 1700
MOUNTAIN STANDARD TIME

Figure 19. Temporal luminescence of Pinus ponderosa and meteorological parameters. Luminescence contrast of background and stressed trees do not correlate with cloud cover conditions cited in figures 17 and 18.

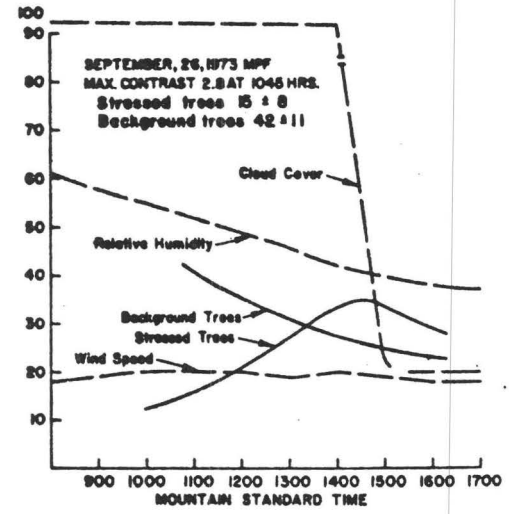
SEPTEMBER, 26, 1973 MPF
MAX. CONTRAST 2.8 AT 1045 HRS.
Stressed trees 15 ± 8
Background trees 42 ± 11
Cloud Cover
Relative Humidity
Background Trees
Stressed Trees
Wind Speed
100
90
80
70
60
50
40
30
20
10
900 1000 1100 1200 1300 1400 1500 1600 1700
MOUNTAIN STANDARD TIME

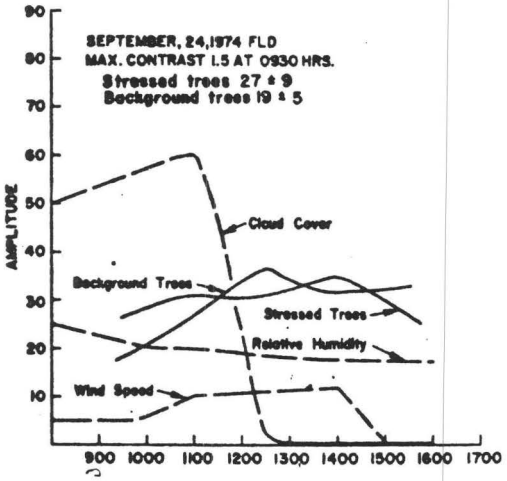
SEPTEMBER, 24, 1974 FLD
MAX. CONTRAST 1.5 AT 0930 HRS.
Stressed trees 27 ± 9
Background trees 19 ± 5
AMPLITUDE
Cloud Cover
Background Trees
Stressed Trees
Relative Humidity
Wind Speed
90
80
70
60
50
40
30
20
10
900 1000 1100 1200 1300 1400 1500 1600 1700

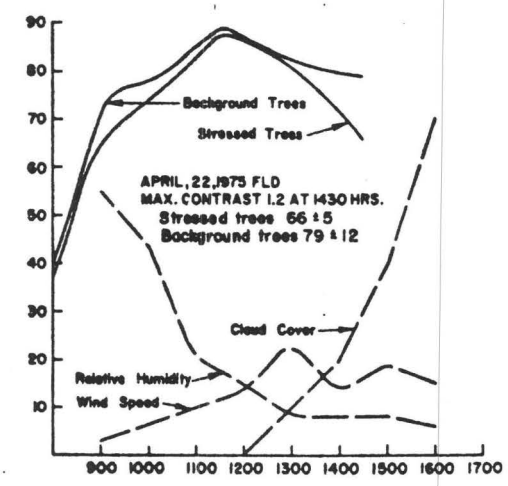
Background Trees
Stressed Trees
APRIL, 22, 1975 FLD
MAX. CONTRAST 1.2 AT 1430 HRS.
Stressed trees 66 ± 5
Background trees 79 ± 12
Cloud Cover
Relative Humidity
Wind Speed
90
80
70
60
50
40
30
20
10
900 1000 1100 1200 1300 1400 1500 1600 1700

In addition to Pinus ponderosa, luminescence measurements were also made July 25, 1974 and May 6, 1975 on trees growing in soils containing background and anomalous concentrations of molybdenum 17 kilometres (km) southeast of Gardnerville, Nevada (Fig. 20). Country rock includes limestone, monzonite, and volcanic rocks of Triassic to Jurassic age. Trees in the area are limited to pinon pine (Pinus monophylla) and juniper (Juniperus utahensis). In the 1974 measurements, the standard derivation of FLD luminescence counts for pinon pine commonly exceeded the value of the mean; this is also attributed to viewing background soil and grass through the low density pine foliage similar to the experience described above. By restricting FLD observations on both dates to denser junipers, standard deviation, rarely exceeded 7 percent of the mean. Molybdenum content in plant ash of 32 juniper trees in Figure 20 are shown in Table 4. Figure 21 shows a linear regressive analysis correlating luminescence counts on both dates with molybdenum in concentrations of 20 to 300 ppm. Correlation coefficients are 0.73 for the July 1974 data (17 trees) and 0.80 for the May 1975 data (17 trees) at confidence levels of 99.97. Luminescence measurements were not performed on all 32 trees because of small size and low foliage density of some individuals, and because some grew in places difficult to approach with the helicopter.

The 1975 data were measured at 10:00. Repeated measurements on 12 stressed and background trees at 12:00 and 15:00 hours showed marked diurnal consistency. For example, mean FLD count for background trees increased from 53 to 10:00 a.m. to 58 at noon, and decreased to 49 at 15:00. Mean FLD count for stressed trees showed even less variation, increasing from 37 to 10:00 to 39 at noon, and decreasing to 35 at 15:00. The 1974 data also appear to be diurnally consistent, although because of high winds and helicopter engine power problems, earlier data were not acquired sequentially and the time of each measurement was not recorded.

Figure 20. Location of geochemically stressed and background trees in the Alpine Mill area, about 17 km southeast of Gardnerville, Nevada. Background trees are arbitrarily denoted as those containing 70 ppm molybdenum or less.

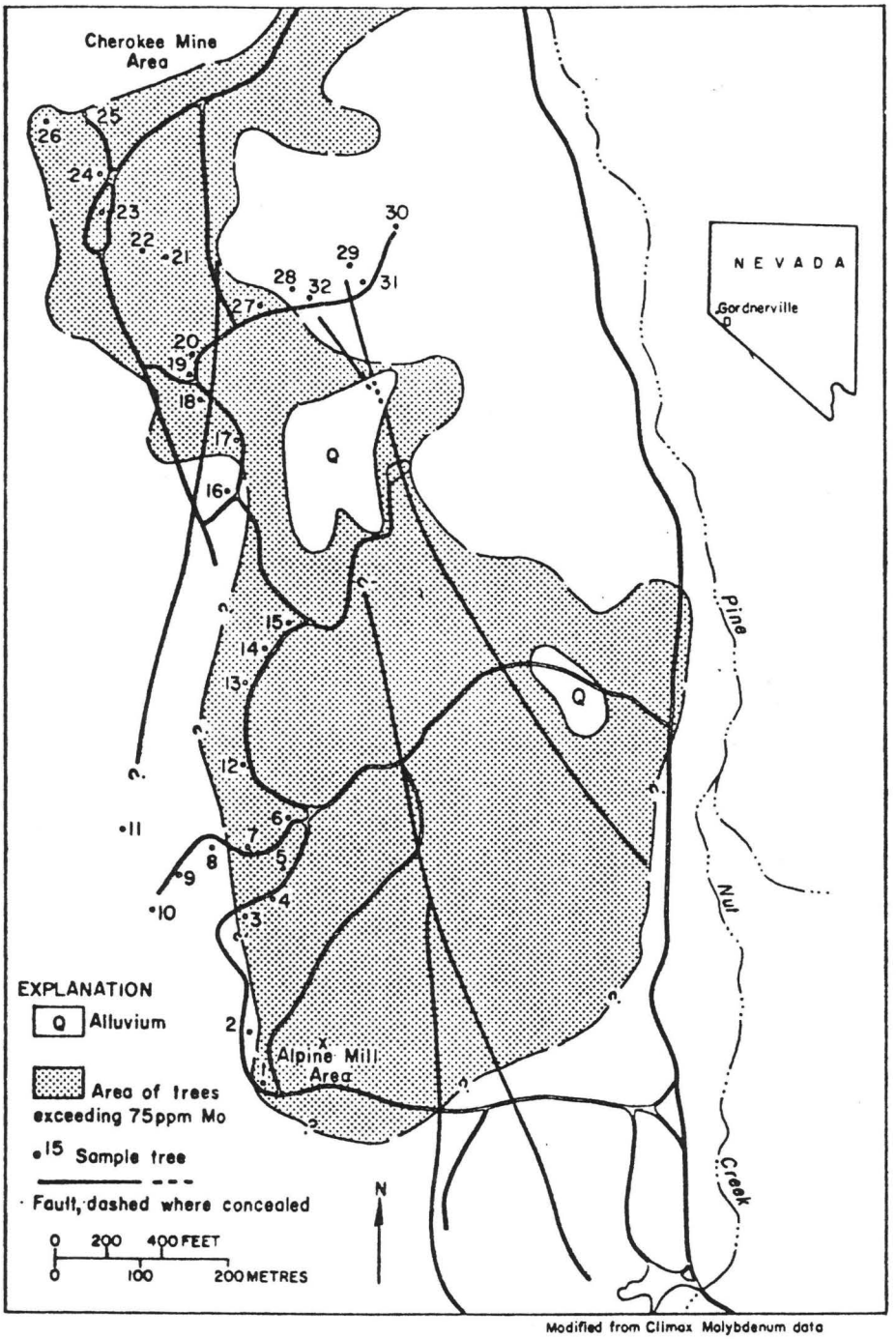

Modified from Climax Molybdenum data

Table 4. Location, molybdenum content (ppm) in ash, and luminescence, expressed in rhodamine WT equivalence (ppb), of geochemically stressed and background trees in the Alpine Mill area. Background trees are arbitrarily denoted as those containing 70 ppm molybdenum or less.

Tree Number	Molybdenum content	Luminescence
1	150	0.69
2	50	1.60
3	300	0.73
4	500	0.56
5	500	(not measured)
6	300	0.20
7	500	0.74
8	20	(not measured)
9	30	(not measured)
10	70	1.02
11	50	0.87
12	200	0.33
13	500	0.53
14	500	0.26
15	70	0.92
16	50	(not measured)
17	100	(not measured)
18	500	0.18
19	150	0.33
20	200	0.38
21	500	0.57
22	500	0.58
23	100	0.21
24	200	0.51
25	70	(not measured)
26	150	0.27
27	200	0.38
28	30	1.09
29	70	0.75
30	30	0.87
31	20	(not measured)
32	50	(not measured)

Figure 21. Linear regressive analysis correlating FLD luminescence counts for specific trees with molybdenum concentrations from 20 to 300 ppm.

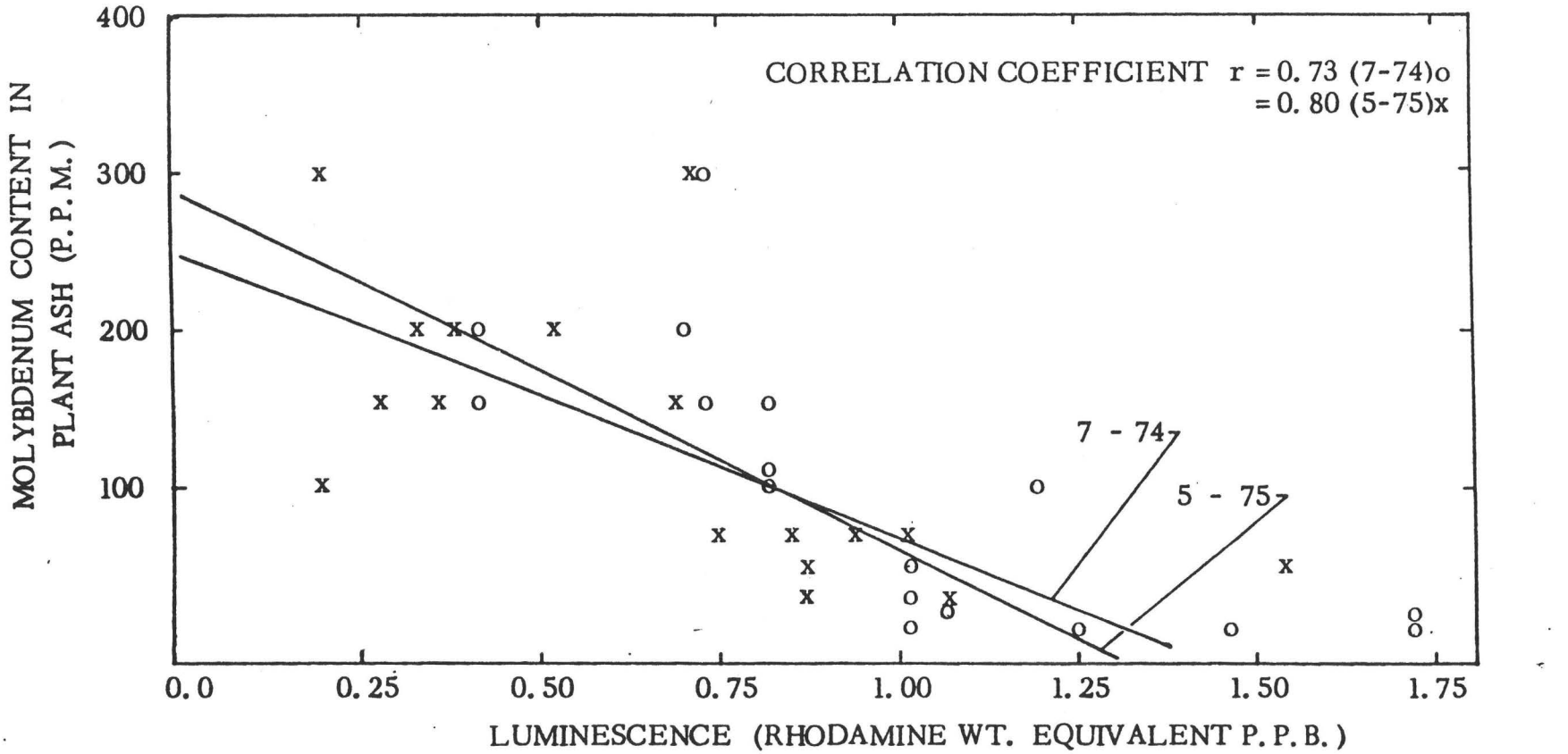
CORRELATION COEFFICIENT r = 0.73 (7-74)o
= 0.80 (5-75)x
7 - 74
5 - 75
MOLYBDENUM CONTENT IN PLANT ASH (P.P.M.)
400
300
200
100
0.0
0.25
0.50
0.75
1.00
1.25
1.50
1.75
LUMINESCENCE (RHODAMINE WT. EQUIVALENT P.P.B.)

Both the 1974 and 1975 data show a decrease in luminescence of juniper with an increase in molybdenum.

Although these results show correlation of luminescence and geochemically induced plant stress for only two species, Pinus ponderosa and Juniperus Utahensis, it is possible that luminescence may vary diurnally and seasonally with species; for example, although Pinus ponderosa showed marked diurnal variability, Juniperus utahensis was remarkably consistent during the days these trees were measured. A practical approach may be to restrict analyses of luminescence of geochemically stressed plants to single specie areas, or to one or two species in mixed groups. Additional work is required to understand variation of diurnal and seasonal luminescence with species.

Phosphate rock

Sedimentary phosphate rock is an increasingly important raw material for production of agricultural fertilizer. A common problem in prospecting for this material, however, is that cursory field observation reveals few physical properties which distinguish phosphatic from non-phosphatic beds. Although small hand-carried ultraviolet lamps have been used to stimulate luminescing minerals and rocks, these methods of prospecting are limited because the lamps are low powered, effective range is limited to a metre or less, and the work must be conducted at night because the low intensity luminescence is obscured by bright sunlight.

To assess the application of the FLD in prospecting for phosphate rocks, the luminescence of ten samples of sedimentary phosphate rocks from several geographic locations, measured with the laboratory fluorescence spectrometer at the 486.1 nm Fraunhofer line, are shown in Table 6. All samples luminesced within the sensitivity range of the FLD, and pointed to the need for a field test.

Several deposits of commercial grade phosphate occur in southern California (Gower and Madsen, 1964). One of the highest grade deposits occurs near Pine Mountain, northeast of Santa Barbara, in the upper part of the Santa Margarita Formation of Miocene age (Fig. 22) where a phosphate zone more than 24 metres thick occurs in siltstone and siliceous shale.

Table. 6. Luminescence of 10 phosphate samples measured with the laboratory fluorescence spectrometer at 486.1 nm in terms of rhodamine WT equivalence (source-detector, solar, and depth corrected).

	Luminescence (ppb)
Blue apatite from Brazil (low F_2, high rare earths)	8.0
Cunday, Colombia (25% P_2O_5, 2% F_2, 100 ppm rare earths)	7.9
Monterey, California pelletal phosphate (25% P_2O_5, 2-3% F_2, rare earths present)	6.5
Tennessee brown phosphate (30%+ P_2O_5, 3% F_2, rare earths unknown)	5.4
Diammonian phosphate-aqueous $NH_4O_4+H_3PO_4$ (N(15%)-P(53%)-K(0%), Ø F_2	3.8
Cook Hollow, Tennessee (reprecipitable phosphate, low rare earths)	2.9
Triple super phosphate $Ca_xH_yPO_4$ (N(0%)-P(48%)-K(0%) some F_2)	2.8
Homeland Mine, Florida (35% P_2O_5, 3.5% F_2, 200-300 ppm rare earth)	1.6
Manatee County Florida red phosphate (30% P_2O_5, 3% F_2)	0.7
North Carolina TGS 16 heavy fraction (30% P_2O_5, 3.5% F_2, 200 ppm rare earths)	0.4

Figure 22. Geologic map of part of the Sespe Creek area (Vedder, Dibblee, and Brown, 1973) showing location of a helicopter traverse (solid line east of Chorro Grande Canyon), and helicopter hovers (A through D). Numbers along traverse are FLD luminescence counts.

Excitation spectra of gypsum and phosphate rock and soil samples from the Santa Margarita Formation measured on the laboratory fluorescence spectrometer show that luminescence at the 486.1 nm Fraunhofer line exceeds luminescence measured at 589.0 and 656.3 nm lines. Table 7 shows that the luminescence of the phosphate and gypsum samples appear to be within the sensitivity limits of the FLD.

Table 7. Luminescence of phosphate and gypsum samples, collected from the Santa Margarita Formation near Pine Mountain, California, and measured with the MPF-3 at 486.1 nm in terms of rhodamine WT equivalence (source-detector, solar, and depth corrected).

Sample	Luminescence (ppb)
Phosphate pellets	0.37-1.05
Phosphate soil	0.33
Gypsum	0.65
Gypsum soil	0.53
Assorted samples from nonphosphatic rocks (Tmv and Ts, fig. 22)	0.22-.34

Two experiments were conducted to measure these materials in the field. Through a cooperative arrangement with the Geological Survey's Water Resources Remote Sensing group in Prescott, Arizona, the Perkin-Elmer FLD was flown aboard their HUlB helicopter over the Sespe Creek area on November 26, 1974, at a hover altitude of 50 metres. Reflectance and luminescence of gypsum, phosphate rock and soil, background soil and vegetation along Chorro Grande Canyon are shown for the 486.1 nm Fraunhofer line in Table 8. Although both gypsum and phosphate are luminescent, the two are significantly different in reflectance so that it is possible to distinguish them.

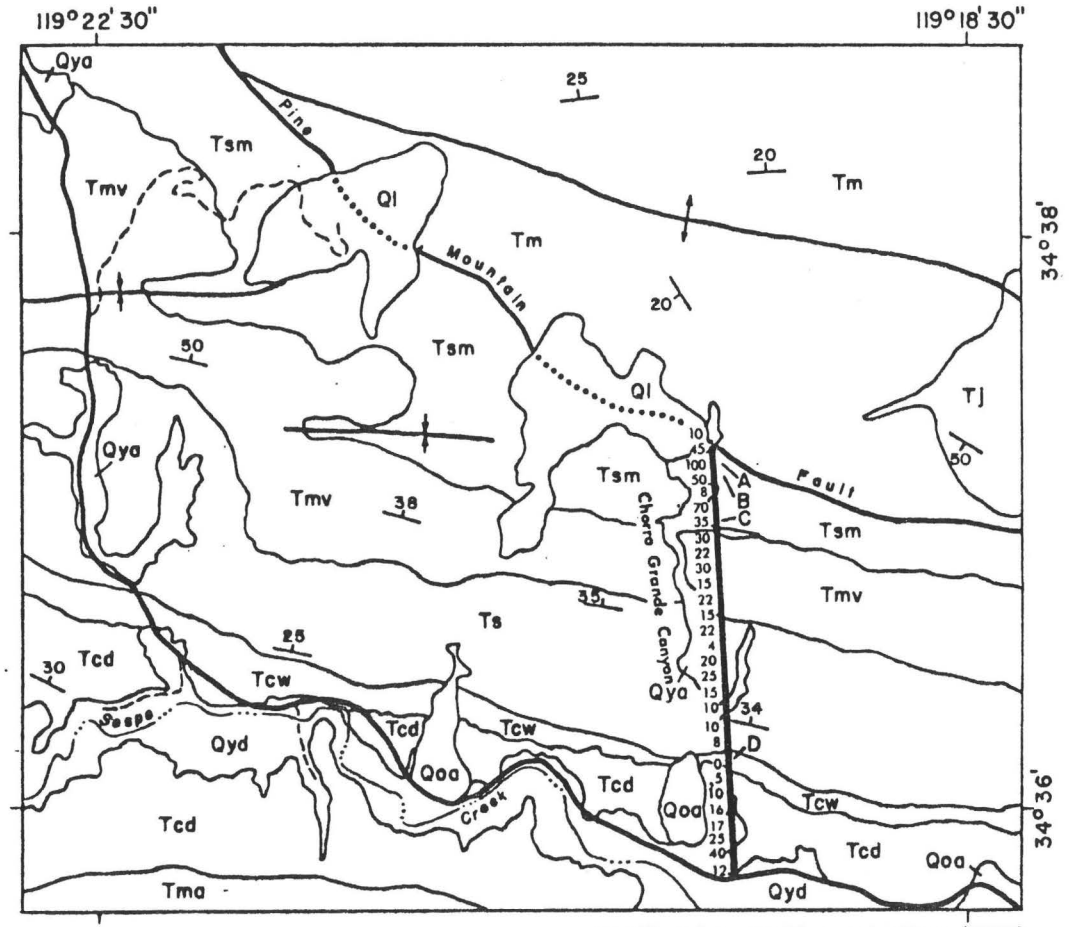

EXPLANATION

QUATERNARY

Holocene

Qya — Younger alluvium

Ql — Landslide deposits

Pleistocene

Qoa — Older alluvium

UNCONFORMITY

TERTIARY

Miocene

Tsm — Santa Margarita Formation

Tmv — Monterey Shale, Rincon Mudstone, and Vaqueros Formation, undifferentiated

Oligocene(?)

Ts — Sespe Formation

Eocene(?)

Tcw — Coldwater Sandstone

Eocene

Tcd — Cozy Dell Shale

Tm — Matilija Sandstone

TJ — Juncal Formation

Contact

Fault trace, dotted where concealed

Anticline, showing crestline

Syncline, showing troughline

34 — Strike and dip of beds

Table 8. Reflectance, FLD counts, and luminescence in terms of rhodamine WT equivalency (source-detector, solar, and depth corrected) of phosphate, gypsum, and background reference materials. Field FLD measurements were performed in November, 1974.

Sample	Reflectance	FLD counts	Luminescence ppb
Gypsum	0.2253	68 ± 5 (66 ± 2)	1.16
Phosphate rock and soil	0.0471	52 ± 3 (43 ± 2)	0.95
Gray card		0 ± 3 (0 ± 1)	0.26
Background soil and vegetation		3 ± 1	0.30
Average of 10 readings from Tmv and Ts (figure 22)		16 ± 4	.46

Values in parenthesis in Table 8 were obtained by placing samples of the phosphate and gypsum under the FLD in a static ground measurement test. Agreement between the flight and static techniques is good, with a larger standard deviation occurring in the airborne helicopter measurements because of the nonhomogeneity of outcrops, soil, and vegetation in the FLD field of view. A calibration figure of 1.32 ppb/100 counts (see Section 5) was used to convert airborne counts to rhodamine WT equivalence.

This experiment was repeated May 8, 1975 with a commercial rental Bell Jet Ranger helicopter at alitudes of 35 m for hover and 150 m for traverse. FLD counts for a single traverse are shown along the bold north-south line in figure 22. The counts are substantially higher in the Santa Margarita Formation than in the less phosphatic older rocks. In addition, luminescence and reflectance of gypsum, phosphate rock, phosphate soil, background sandstone, and background grass and soil were determined by

hovering over each material along Chorro Grande Canyon (points A, B, C, and D, figure 22) and collecting approximately 50 data points for each material. Reflectance, FLD counts, and rhodamine WT equivalent luminescence for two hover runs over Chorro Grande Canyon are shown in Table 9.

Comparison of Tables 8 and 9 show that relative values of reflectance and luminescence for gypsum and phosphate correlate well for both dates, although the 1975 data are higher; background grass and soil are substantially higher. These increased levels of luminescence could be due, in part, to greater insolation in May than in November. The differences could also be attributed to the fact that 1974 and 1975 hovers were in the same area but over slightly different outcrops. Comparison between values of rhodamine WT equivalency calculated from FLD counts (Tables 8 and 9) and those values based on measurements with a laboratory fluorescence spectrometer (Table 7) shows that higher values were obtained for luminescence of phosphate from the spectrometer than with the FLD. This is probably caused by phosphate content of the pellet sample measured with the laboratory spectrometer being higher than the bulk phosphate rock measured with the FLD in the field. It is not understood why the luminescence level of gypsum measured with the FLD exceeds the level measured with the laboratory spectrometer by nearly a factor of 2.

In addition to the measurements noted above, phosphate rock was measured with the FLD during a series of airborne experiments in the Lakeland, Florida area. The materials measured had been mined and are therefore not representative of weathered surfaces on natural outcrops as in the case of the California phosphate. Luminescence of these materials is shown in Table 10.

Table 9. Reflectance, FLD counts (mean and standard deviation of the mean), and luminescence in terms of rhodamine WT equivalency of phosphate, gypsum and background materials. Airborne field FLD measurements were performed May 8, 1975.

	Run 1			Run 2		
Sample	Reflectance	FLD counts	Luminescence rho. WT ppb	Reflectance	FLD counts	Luminescence rho. WT ppb
Gypsum (hover A)	.1114	97 ±5	1.54	.0948	92 ±15	1.47
Phosphate rock and soil (hover B)	.06	77 ±7	1.28	.051	72 ±8	1.21
Phosphate soil (hover C)	.042	56 ±6	1.0	.045	64 ±8	1.10
Sandstone (hover D)	.082	41 ±4	0.80	.147	50 ±11	0.90
Background grass and soil	.041	35 ±2	0.72	.052	21 ±3	0.52
Gray card		0 ±5	0.26		0 ±4	0.26

Table 10. FLD counts (mean and standard deviation of the mean) and luminescence in terms of rhodamine WT equivalency of associated phosphate and gypsum materials in the Lakeland, Florida area.

Source	FLD counts	Luminescence rho. WT ppb
Gray card	0±2 (overcast)	0.26
	2±3 (clear sky)	0.29
Phosphate venier in dredged pit	65±12 (overcast)	1.12
Phosphate rock pile (Royster plant)	116±4 (overcast)	1.79
	143±4 (clear sky)	2.15
Gypsum pile	137±4 (overcast)	2.04
	189±15 (clear sky)	2.75

Comparison of the gray card, phosphate rock pile, and gypsum measurements shows that the FLD performs adequately under overcast conditions, although rhodamine WT equivalency for these three materials is reduced 10, 17, and 26 percent, respectively.

Oil spills and seeps

In order to quantify the luminescence of selected oils in terms of rhodamine WT equivalence, the excitation spectra of 29 crude oils and 20 refined oils were measured with the laboratory fluorescence spectrometer by Watson and others (1974). The integrated excitation intensities, corrected for source detector, solar, and depth effects for all samples of crude and refined oils, are shown in Tables 11 and 12.

Table 11. Integrated excitation intensity of crude oils at specific Fraunhofer wavelengths in terms of equivalency with rhodamine WT. Samples are ordered by decreasing intensity at the 486.1 nanometer Fraunhofer line and corrected for source-detector, solar, and depth effects.

SAMPLE	DESCRIPTION		SPECIFIC	WAVELENGTH (NANOMETERS)					
	NO.	NAME	GRAVITY	396.8 (ppb)	422.7 (ppb)	486.1 (ppb)	518.4 (ppb)	598.0 (ppb)	656.3 (ppb)
1C	19327	MICHIGAN	.8327	4.88	12.95	34.62	36.36	20.62	5.95
2C	17394	WYOMING	.7866	4.16	11.51	29.33	30.46	15.90	6.26
3C	31473	WYOMING	.8098	4.86	13.64	26.86	26.36	12.44	3.33
4C	26294	NIGERIA	.8163	6.63	12.33	25.80	22.17	8.76	3.87
5C	24563	COLORADO	.8172	3.16	8.84	22.19	22.63	11.24	4.07
6C	17636	LOUISIANA	.8834	5.84	11.12	16.54	14.84	3.40	2.24
7C	29350-5	DENMARK	.7790	1.21	3.45	14.68	18.16	12.32	5.91
8C	24461	MISSISSIPPI	.7932	2.91	6.74	10.93	10.58	5.90	2.36
9C	31316	CALIFORNIA	.8532	5.52	8.98	8.49	6.91	2.23	0.58
10C	28212	MISSISSIPPI	.8455	1.30	3.28	6.39	5.93	2.74	1.90
11C	31317	CALIFORNIA	.8377	0.71	1.84	6.34	7.77	5.65	2.43
12C	26241	TRINIDAD	.8318	0.76	2.03	6.31	7.22	3.48	1.86
13C	30534-1		.7317	0.93	2.48	6.16	6.89	4.29	1.84
14C	32219	CALIFORNIA	.7713	0.87	2.59	5.76	6.48	3.47	2.16
15C	24569	COLORADO	.8574	1.18	3.74	5.45	10.64	5.19	2.21
16C	27358	LIBYA	.8350	0.88	2.02	5.41	5.66	3.32	1.44
17C	13786	MISSISSIPPI	.8045	0.66	1.74	5.07	6.40	6.93	2.22
18C	27458	CANADA	.7735	1.56	2.80	3.81	3.78	1.90	0.87
19C	31851	BAHRAIN	.8695	0.43	1.16	3.27	3.95	3.44	2.02
20C	30229-1	ALASKA	.8654	0.35	0.78	2.50	2.91	2.35	0.59
21C	13588	WYOMING	.9110	1.80	2.42	2.33	2.29	1.76	1.09
22C	25968-2	WYOMING	.8430	0.23	0.70	2.10	2.52	1.72	1.27
23C	25179	IRAN	.8854	0.21	0.62	1.74	1.97	1.64	0.84
24C	27173	BAHRAIN	.8370	0.29	0.59	1.72	2.25	2.74	1.23
25C	29619	CALIFORNIA	.8639	0.29	0.66	1.63	1.90	1.44	0.77
26C	27360	LIBYA	.8481	0.41	0.89	1.45	1.60	1.01	0.26
27C	14525	VENEZUELA	.8752	0.28	0.58	1.43	1.06	0.72	0.30
28C	17112	CANADA	.9677	0.09	0.19	0.60	0.78	0.88	0.47
29C	17556	LIBYA	.9312	0.05	0.09	0.22	0.26	0.51	0.05

Table 12. Integrated excitation intensity of refined oils at specific Fraunhofer wavelengths in terms of equivalency with rhodamine WT. Samples are ordered in decreasing intensity at the 486.1 nanometer Fraunhofer line and corrected for source-detector, solar, and depth effects.

SAMPLE	DESCRIPTION	WAVELENGH (NANOMETERS)					
		396.8 (ppb)	422.7 (ppb)	486.1 (ppb)	518.4 (ppb)	589.0 (ppb)	656.3 (ppb)
1R	RPM AVIATION OIL - 100	41.05	90.59	148.09	137.64	37.42	5.34
2R	CHEVRON TURBINE OIL 24 TEP	50.52	70.29	112.29	80.69	15.60	2.50
3R	CHEVRON JOURNAL OIL 80	30.70	58.20	96.19	89.81	68.96	9.97
4R	CHEVRON DELO MARINE OIL SAE 40	42.70	81.13	91.58	62.80	10.20	1.55
5R	CHEVRON MACHINE OIL 19	29.24	59.43	82.58	74.14	26.10	5.26
6R	CHEVRON GEAR OIL 90	30.93	50.66	78.43	83.76	24.17	5.40
7R	CHEVRON COMPRESSOR OIL	41.60	77.86	68.75	38.27	6.40	0.99
8R	CHEVRON DELO CYLINDER LUBRICANT	22.49	49.70	64.97	60.12	15.71	3.02
9R	CHEVRON MARINE OIL 31X	25.00	50.90	57.33	80.47	15.66	3.31
10R	CHEVRON REFRIGERATION OIL 15	42.96	98.91	43.64	16.02	1.68	0.32
11R	CHEVRON DELO CYLINDER OIL 155CX	29.36	88.53	27.78	26.80	15.26	6.26
12R	CHEVRON MULTI-MACHINE OIL SAE 40	21.80	23.11	15.80	10.67	2.06	4.16
13R	CHEVRON VACUUM PUMP OIL	41.90	50.33	14.70	6.43	1.49	4.37
14R	CHEVRON DIESEL FUEL	29.85	29.51	10.11	4.75	0.78	0.27
15R	RPM JET ENGINE OIL 1010	14.37	16.90	9.95	6.15	1.51	1.17
16R	CHEVRON TELEMOTOR OIL 5	17.53	19.32	9.74	7.80	1.52	0.57
17R	CHEVRON CUTTING OIL 210-TA	3.04	5.38	6.16	5.18	2.95	0.71
18R	CHEVRON WHITE OIL 15	0.13	0.22	0.15	0.02	0	0
19R	CHEVRON BASE OIL C	0.07	0.05	0.05	0.06	0.16	0.14
20R	CHEVRON WHITE OIL 3 NF	0.03	0.06	0.02	0	0	0

Results for the crude oils (Table 11) exhibit a peak rhodamine WT equivalency at Fraunhofer wavelengths of 518.4 nm or shorter, with 19 samples (65 percent) having a maximum at 518.4 nm. Luminescence of twenty-eight of the twenty-nine samples exceeds 0.25 ppb rhodamine WT equivalency and appears to be within the sensitivity range of the FLD. Refined oils (Table 12) show a greater range in rhodamine WT equivalency than do the crude oils. Laboratory values for 17 samples (85 percent) show a peak rhodamine WT equivalency at 486.1 nm or shorter, but in this case only seven samples (35 percent) have a maximum at 422.7 nm and one sample (6 percent) has a maximum at 396.8 nm. Seventeen of the twenty samples appear to be within the sensitivity range of the FLD.

Specific gravity of the 29 crude oils ranges from 0.7317 to 0.9677. The dependence of bulk oil luminescence on specific gravity is shown in Figure 23. A regressive analysis was performed on the 29 crude oil samples to obtain the best least-squares fit to the data points, with both the correlation coefficient and the standard error determined for six selected Fraunhofer lines throughout the visible spectrum. Correlation coefficients range from .34 at 656.3 nm to .77 at 396.8 nm and indicate that the best correlation between luminescence and specific gravity occurs at 396.8 nm.

To assess the feasibility of correlating luminescence with oil thickness such as a film of oil in a marine spill, measurements were performed with the laboratory fluorescence spectrometer and with liquid sample holders into which oil films of discrete thickness could be inserted. The sample holders consisted of a quartz substrate approximately 2 cm in diameter, onto one surface of which an aluminum film of either 3 μm (micrometres) or 10 μm was deposited as a ring. The oil sample was placed in the center of the ring the excess thickness removed by positioning a quartz cover plate in firm contact with the aluminum film.

The excitation spectra of six crude oils in 3 μm and 10 μm films and in bulk thickness were measured at six Fraunhofer wavelengths. Table 13 summarizes these results, which are expressed in terms of rhodamine WT equivalency (corrected for source-detector, solar, and depth effects) and listed in order of increasing specific gravity.

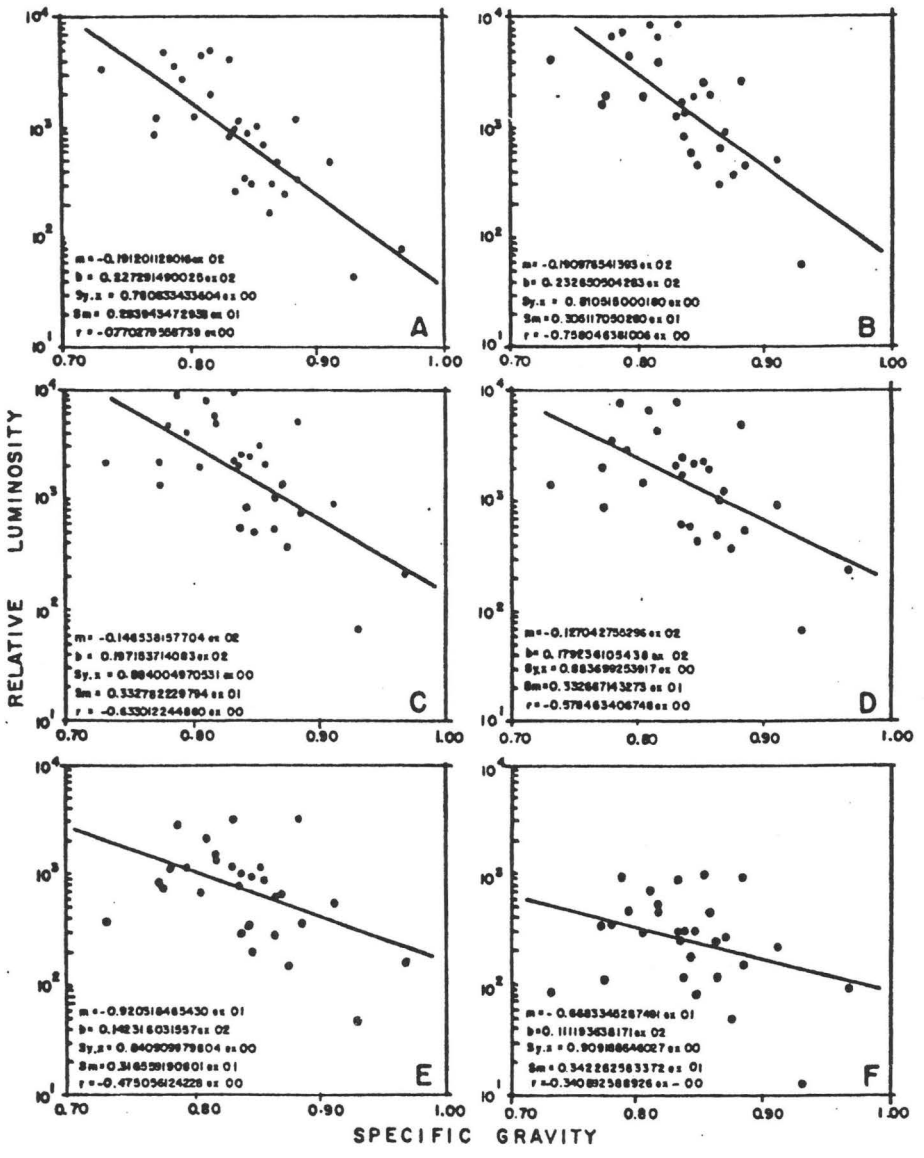

Figure 23. Statistical plot showing correlation between relative luminescence and specific gravity of 29 crude oils at the following Fraunhofer lines: A, 396.8nm; B, 422.7 nm; C, 486.1 nm; D, 518.4 nm; E, 589.0 nm; F, 656.3 nm.

Table 13. Integrated exitation intensity of crude oils and oil films at six Fraunhofer wavelengths in terms of rhodamine WT equivalency. Samples are corrected for source-detector, solar, and depth effects.

SAMPLE	Film Thickness	SP. GR.	WAVELENGTH (NANOMETERS) 396.8 (ppb)	422.7 (ppb)	486.1 (ppb)	518.4 (ppb)	589.0 (ppb)	656.3 (ppb)
13C	Bulk	0.7317	5.52	8.98	8.49	6.91	2.23	.581
	10.0μ		.721	.915	.643	.488	.171	.054
	3.0μ		.372	.503	.310	.217	.124	.075
7C	Bulk	.7790	5.84	11.12	16.54	14.84	3.40	2.24
	10.0μ		2.91	5.38	5.02	3.83	1.19	.286
	3.0μ		1.25	1.95	1.72	1.27	.356	.078
1C	Bulk	.8327	4.88	12.94	34.62	36.36	20.62	5.95
	10.0μ		4.51	10.93	20.53	11.48	3.86	9.76
	3.0μ		1.81	4.29	5.17	4.35	1.28	.318
27C	Bulk	.8752	.279	.581	1.43	1.06	.072	.306
	10.0μ		.224	.488	.914	.984	.054	.271
	3.0μ		.217	.488	.930	1.01	.062	.317
29C	Bulk	.9312	.054	.093	.225	.256	.201	.140
	10.0μ		.054	.078	.194	.194	.178	.147
	3.0μ		.054	.078	.194	.209	.201	.140
28C	Bulk	9677	.093	.186	.605	.775	.884	.473
	10.0μ		.085	.171	.666	.837	.814	.521
	3.0μ		.078	.163	.620	.798	.760	.506

Table 13 suggests the following:

1. The luminescence of the 3 μm and 10 μm films of the lower specific gravity oils (0.7317) to 0.8327) is significantly less than that of the bulk oil.

2. At specific gravities of 0.8752 or greater, luminescence of the film approaches that of the bulk oil.

3. The peak luminescence of the 3 μm and 10 μm films shows a spectral shift toward the blue end of the wavelength spectrum for the low specific gravity oils and toward the red end of the spectrum for the higher specific gravity oils.

4. Comparison of luminescence of the 3 μm and 10 μm films at the six Fraunhofer wavelengths suggest that the thickness of an oil film can be determined for specific gravities of 0.8327 and lower.

5. For oils of specific gravity of 0.8752 and heavier, the difference in luminescence between the film and bulk oil is negligible.

Natural fractures in the ocean floor of the Santa Barbara Channel, California permit oil of varying densities to seep to the surface. Throughout the Channel, patches of oil films at various times can be seen with the naked eye. At times heavy crude seeps form narrow filaments near Coal Oil Point that extend for several miles parallel to the shore line.

To measure the luminescence of crude oil with the prototype FLD, a sample of oil from the Santa Barbara Channel was poured into a tank of water; luminescence of the resulting film was not detected (Hemphill and others, 1969); because 1) the emission peak of the Santa Barbara oil is at a shorter wavelength than 589.0 nm where the prototype FLD operated and 2) sensitivity of the prototype FLD was inadequate.

Luminescence of oil seeps off Coal Oil Point were measured during the week of November 24, 1974 with the redesigned FLD operating from a helicopter at the 486.1 nm Fraunhofer wavelength. Use of optical gain techniques described in sections 4 and 8 was necessary to offset the dynamic range problem encountered when measuring material of very low reflectance. Mean and standard deviations in luminescence for the November measurements are shown in figure 24.

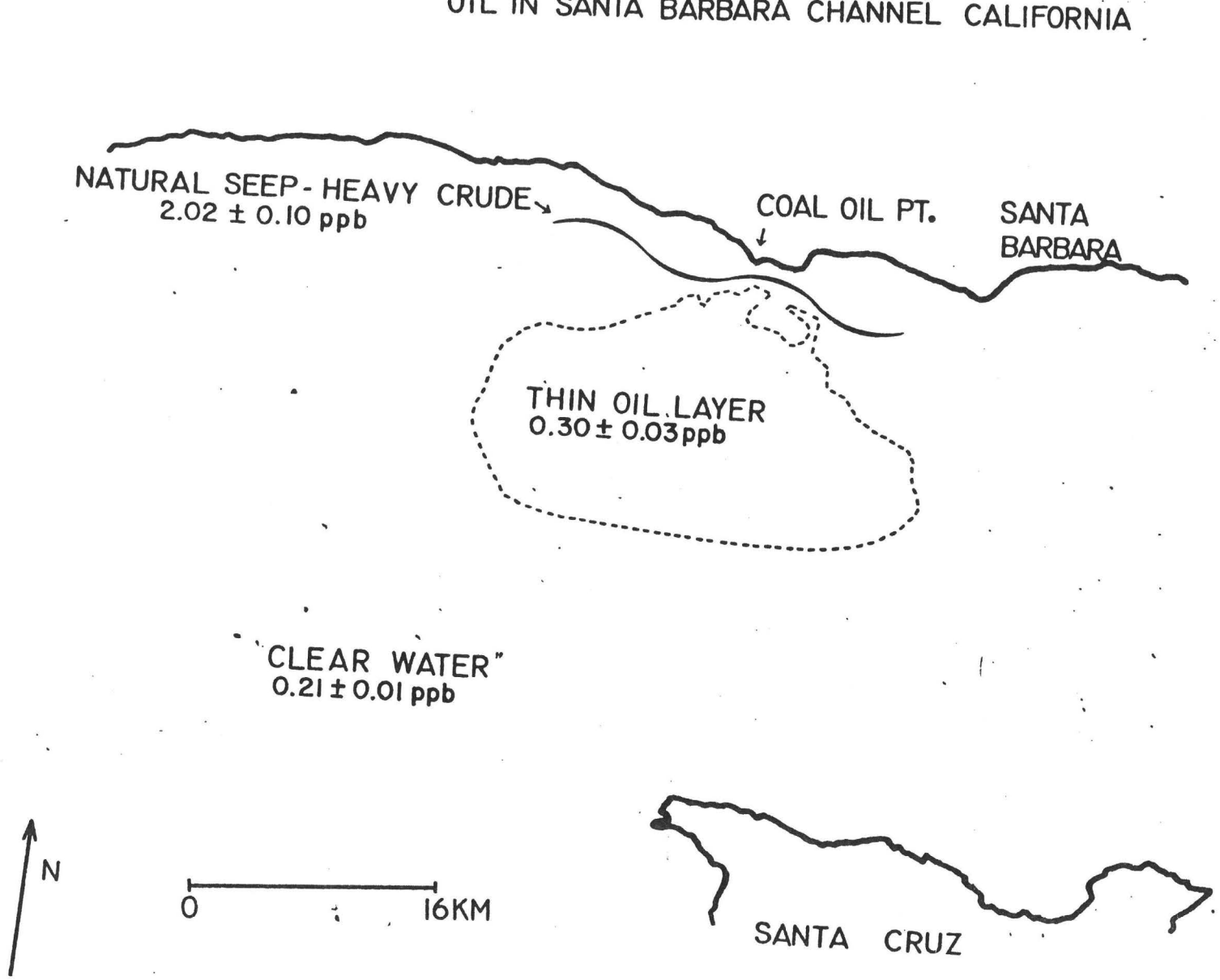
OIL IN SANTA BARBARA CHANNEL CALIFORNIA
NATURAL SEEP - HEAVY CRUDE
2.02 ± 0.10 ppb
COAL OIL PT.
SANTA BARBARA
THIN OIL LAYER
0.30 ± 0.03 ppb
CLEAR WATER"
0.21 ± 0.01 ppb
N
0
16KM
SANTA CRUZ

Figure 24. Map showing 1) dispersal of oil from natural seep off Coal Oil Point, Santa Barbara Channel, and 2) FLD luminescence responses from clear water, thin oil film, and heavy crude filament.

The relatively large standard deviations encountered for both clear water and thin oil layers are believed to be due to alternating small areas of thin oil and clear water throughout the Channel that are included in both measurements. This problem of alternating target intensities was not encountered in the measurements on the denser and thicker crude oil layers. Luminescence intensities of small lakes several miles inland from the coast average 20-40 counts less than the counts of so-called "clear" Santa Barbara Channel water, suggesting that small amounts of oil or other luminescing material is present in the Channel.

Lignin sulfonate

Spent sulfite liquor is produced as a waste material in the process of making paper from wood pulp. Disposal of the material into rivers and estuaries constitutes a severe water pollution problem in areas where numerous paper mills are located. The spent sulfite liquors are injurious to fish due to the high oxygen demand of the liquors (T. Almgren and B. Josefsson, 1973).

Lignin sulfonate is a constituent of the liquor that exhibits inherent luminescence. Christman and Minear (1967) observed that both pure lignin sulfonate and whole spent sulfite liquor, collected from three localities, exhibited identical excitation and emission peaks at 340 nm and 400 nm, respectively. The relation between luminescence intensity and concentration of the whole waste liquor was linear for the samples studied. H. F. Smith and P. S. Flandreau (Perkin-Elmer Corporation, written commun., 1969) observed a slight shift of the emission peak of sulfite liquor towards shorter wavelengths as the concentration of the liquor in the water was reduced. They also noted that changing the pH of the solution from acidic to basic was accompanied by both a reduction in emission intensity and a 20 nm to 40 nm shift in the emission peak toward longer wavelength. Kullbom, Smith, and Flandreau (1970) measured the luminescence of lignins in whole spent liquors from both the "sulfite process" and the "Kraft process." They show that Kraft liquor exhibits a higher luminescence than sulfite liquor but at a shorter peak emission wavelength. Kraft liquor has a peak emission of 340 nm compared to 380 nm for sulfite liquor.

In order to predict the luminescence of sulfurized liquor that could be measured with the FLD, excitation spectra of samples of spent liquor were

collected at the Buckeye Cellulose plant, Foley, Florida[1/]. The plant, which is located on the Fenholloway River, has a series of oxidizing lagoons and a final stage waste treatment, the residue from which is dumped into the river. Samples are collected as shown in figure 25 on the river at the upstream side of the plant, at the clarifier pond, at the outlet of the west oxidation lagoon, and on the river at the downstream side of the plant.

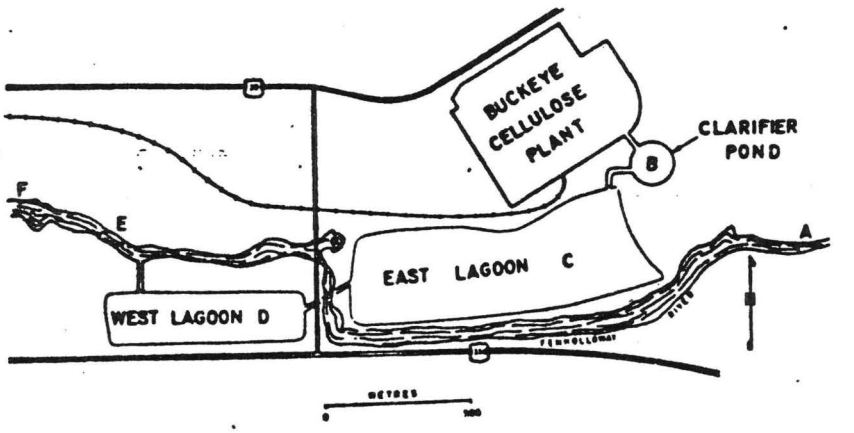

Figure 25. Map showing Buckeye Cellulose plant, and locations A through F where FLD measurements were made. Results are shown in Table 14.

Excitation spectra of sulfurized liquor were measured with the MPF-3 excitation monochromator operating in the scanning mode and the emission monochromator centered at the 486.1 and 589.0 nm Fraunhofer lines. These spectra clearly show a greater response at 486.1 nm than at 589.0 nm (fig. 26)

[1/] The help of the Buckeye Cellulose Corporation is gratefully acknowledged.

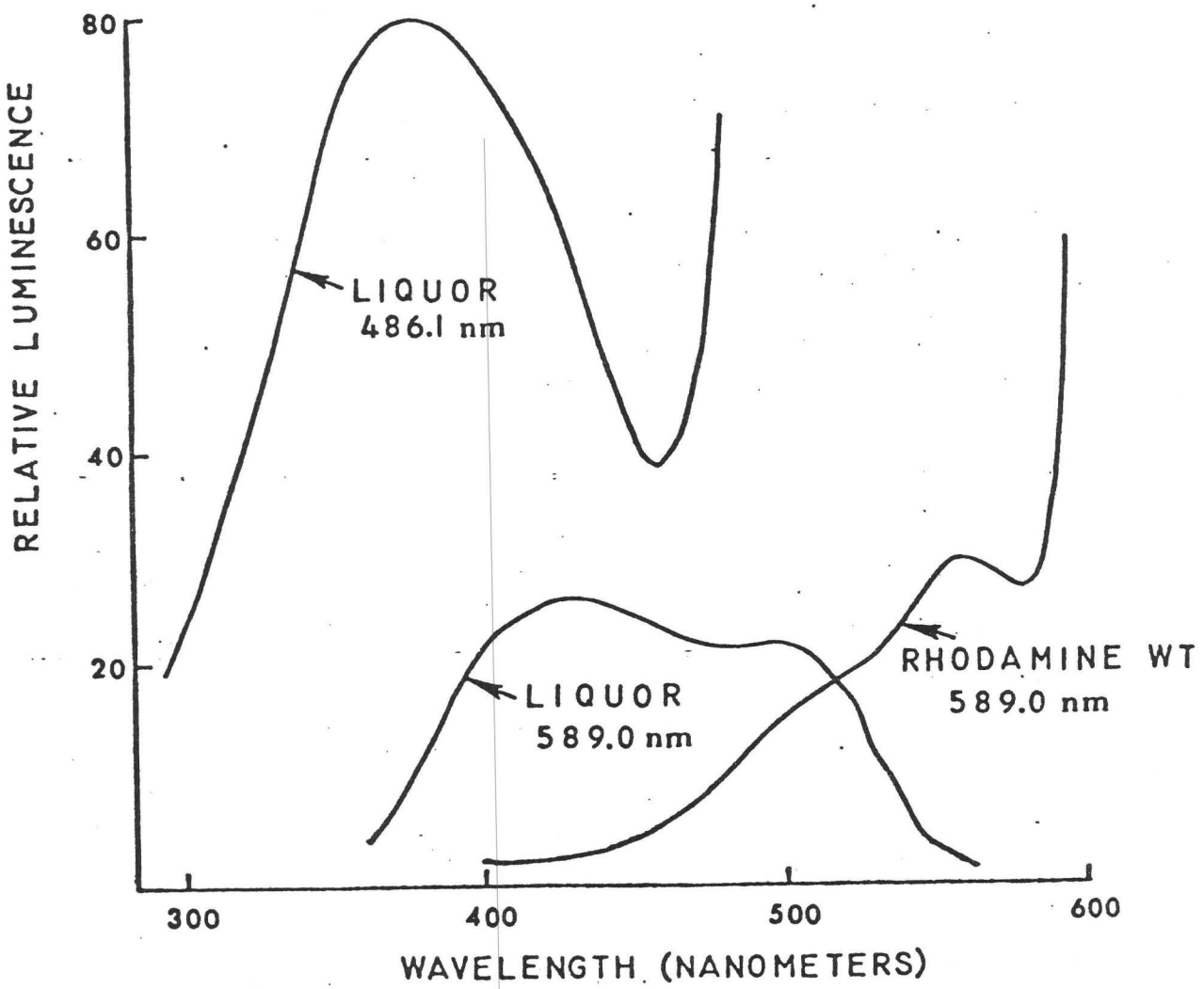

Figure 26. Spectra of sulfurized liquor and rhodamine WT dye measured on the MPF-3 fluorescence spectrometer. Sample was collected from the clarifier pond at the Buckeye Cellulose plant, Foley, Florida.

The sulfurized liquor spectra at 486.1 nm were then solar corrected and depth corrected to 4.0 cm as determined from attenuation measurements in the laboratory (see section 3). Table 14 shows luminescence of the sulfurized liquor measured with the MPF-3 in terms of rhodamine WT equivalency. The sulfurized liquor was predicted to be within the sensitivity limit of the FLD operating at 486.1 nm.

Table 14. Luminescence at 486.1 nm of sulfurized liquor and background materials in the vicinity of the Buckeye Cellulose plant, Foley, Florida in terms of MPF-3 rhodamine WT equivalency, FLD counts, and FLD rhodamine WT equivalency. Location of measurements A through F are shown in figure 25.

Source	MPF-3 rho. equiv. (ppb)	FLD counts	FLD rho. equiv. (ppb)
Gray card		0±3	.25
Non-luminescent standard		0±3	
Background grass and soil		0±3	.26
River (upstream) (A)	.26	0±2	.26
Clarifier pond (B)	.88	54±4	.97
West oxidizing lagoon (C)		145±7	2.17
East oxidizing lagoon (D)		129±7	1.96
River (downstream of plant outlet) (E)	.33	7±1	.35
River (downstream several hundred metres) (F)		5±3	.33

In January 1975, the waste liquor effluent from the Buckeye Cellulose plant, Foley, Florida, was measured with the FLD operating at 486.1 nm, and the helicopter hovering 30 metres over sampling points shown in figure 11: A) the Fenholloway River at the upstream side of the plant, B) clarifier pond (lift) station, C) east oxidizing lagoon, D) west oxidizing lagoon, E) the river at the west lagoon outlet, and F) the river several hundred yards downstream from the plant. Results are summarized in Table 14, both in terms of luminescence counts and equivalent ppb rhodamine WT dye. Measurements were made under overcast sky conditions. Although a slight increase

in luminescence was detected downstream from the plant relative to the oxidizing lagoons, the river showed little luminescence; this suggests that treatment facilities are effective. A comparison between predicted and measured luminescence indicates that the technique of predicting luminescence detectivity with the FLD from laboratory measurements is reliable.

Determination of the concentration of lignin degradation products in the areas measured with the FLD is complicated by the chemistry of the Kraft waste liquor. Lignin products are a class of chemical compounds optically similar to tannic acid. One calibration technique used by the Environmental Protection Agency and by industry is to optically compare the waste liquor to tannic acid and combine them into a category called "equivalent tannic acid." The photometric absorption of a sample of waste liquor is compared with known standards of tannic acid and the equivalent concentration of tannic acid determined. This procedure was followed in determining the equivalent tannic acid concentration for samples at Foley, Florida.[2/] In addition, known concentrations of samples of waste liquors (with tannic acid determined) were measured on the MPF-3 and the relation of equivalent tannic acid concentration (ppm) to rhodamine WT concentration (ppb) determined (fig. 27). From this curve, the "equivalent tannic acid concentration" for each FLD measurement was calculated (Table 15).

It appears from these results that the Fenholloway River has a high background equivalent tannic acid concentration upstream of the plant and that the plant is adding approximately 20% to the total concentration of the river.

[2/] Determined by EPA National Field Investigations Laboratory, Denver, Colorado.

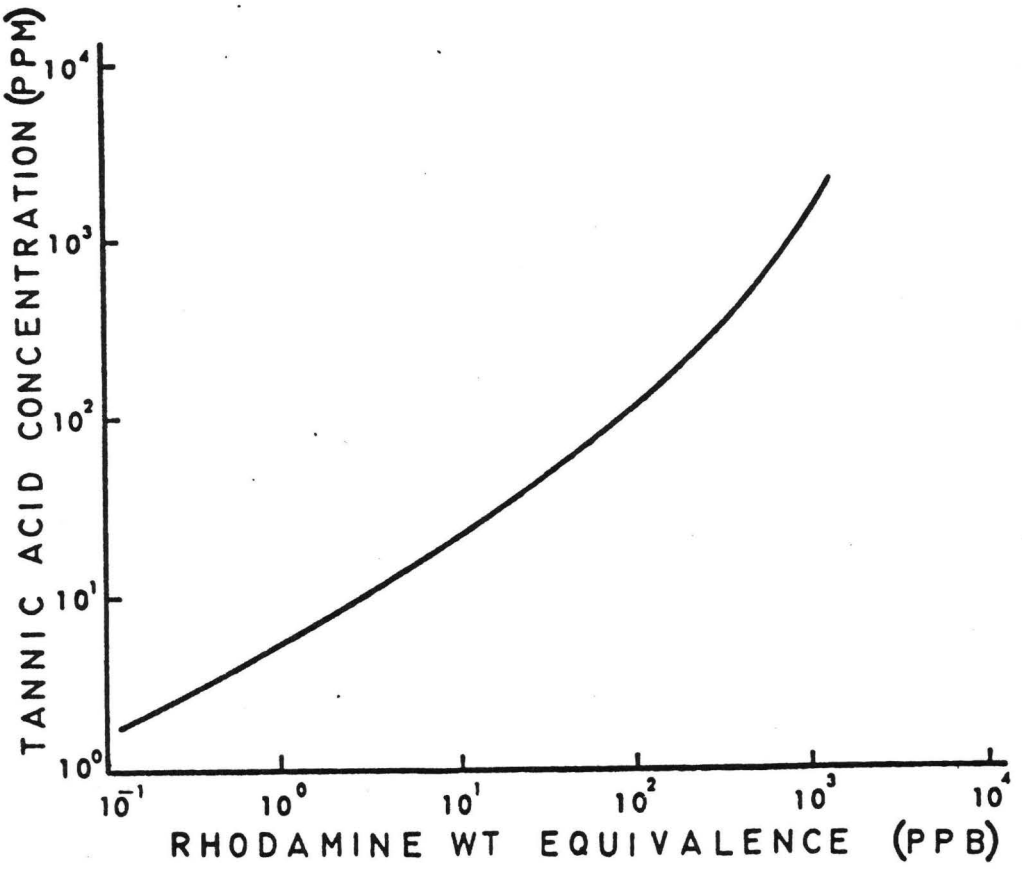

Figure 27. Tannic acid concentration (ppm) plotted as function of rhodamine WT equivalency (ppb).

Table 15. Equivalent tannic acid in parts per million for waters in the vicinity of the Buckeye Cellulose plant, Foley, Florida. Measurement locations are shown in figure 25.

Source	Rhodamine WT equivalency	Tannic acid concentration
River (upstream) (A)	0.26	3.2 ppm
Clarifier pond (B)	0.97	7.2
West oxidizing lagoon (C)	2.17	10.5
East oxidizing lagoon (D)	1.96	9.8
River (downstream of plant outlet) (E)	0.35	3.9
River (downstream several hundred metres (F)	0.33	3.6

Phosphate processing plant effluents

The occurrence of radioactive materials in mined phosphate rock can contribute to severe environmental problems. Uranium concentration varies directly with phosphate concentration, and through radioactive decay radium is produced. Maximum permissable concentration of radium 226 is an order of magnitude less than other decay isotopes because it is the most hazardous water pollutant (Environmental Protection Agency, 1973). Radium 226 decays into radon 222 which in turn decays into products that have been implicated in an increased incidence of lung cancer in workers exposed to high levels. All of these materials are released during the processing of phosphate rock.

Comprehensive information on the milling of phosphate rock and production of phosphoric acid and fertilizers are found in a number of articles (Waggaman, 1952; Ruhlman, 1958; Waggaman and Ruhlman, 1960; Environmental Protection Agency, 1973). Mining techniques vary depending upon geological and hydrological conditions of the locality. In Florida, land pebble phosphate deposits are mined by large electric draglines. The overburden is removed and the ore slurried and pumped to washing plants. Particles less than 200-mesh are discharged from the washing plant to a slime pond. Slime slurry is extremely difficult to treat or dewater, and breaks in slime pond dikes constitute a potential source of ground water pollution. Material larger than 200-mesh is treated in an amine flotation circuit. Silica sand is separated and either slurried to sand piles or placed in mined-out areas. The spent amine flotation water is discharged to mined-out areas and recycled. Following mining and amine flotation, the phosphate rock is either acid treated or thermally reduced. A by-product of this acid treatment is gypsum, which contains radium waste (Environmental Protection Agency, 1973, p. 10). This material is slurried and discharged to

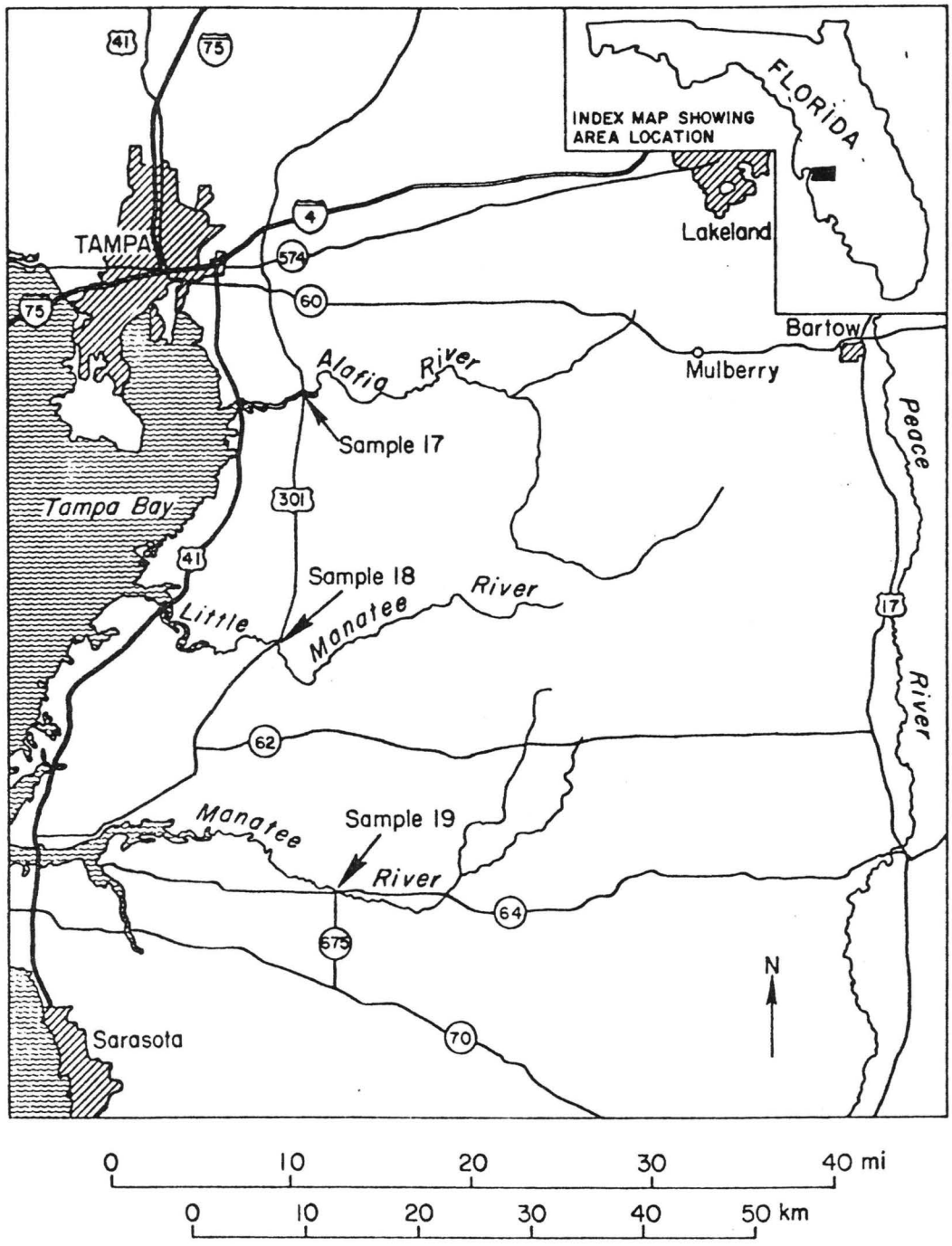
INDEX MAP SHOWING
AREA LOCATION
FLORIDA
Lakeland
41
75
TAMPA
4
574
60
75
Bartow
Alafia River
Mulberry
Sample 17
Peace
Tampa Bay
301
41
Sample 18
Little
Manatee
River
17
River
62
Manatee
Sample 19
River
64
575
N
Sarasota
70
0
10
20
30
40 mi
0
10
20
30
40
50 km

a gypsum pile, where the clarified water is decanted and recirculated to clurry directly into surrounding rivers (Environmental Protection Agency, 1973, p. 11). The gypsum piles are surrounded by a drainage ditch which can overflow or break during heavy periods of rainfall and become a source of water pollution (Environmental Protection Agency, 1973, p. 23). In addition, the bottoms of recycling ponds in Florida consist of an artesian limestone aquifer which, in turn, overlies the Floridian aquifer. Reaction between the acidic gypsum transport water and the limestone aquifer, together with solution cavities in the aquifer, has resulted in the movement of highly radioactive water into the shallow ground water and constitutes a serious source of pollution (Environmental Protection Agency, 1973, p. 25).

To determine the feasibility of detecting phosphate processing effluent with the FLD, samples were collected from surface drainage adjacent to settling pond dikes of processing plants near Mulberry in central Florida (figure 28). Reference samples from outside the phosphate area were also collected from the Alafia, Little Manatee, and Manatee Rivers, 37, 46, and 58 km respectively from the plant area. Table 16 shows luminescence intensi of the samples at six Fraunhofer wavelengths. Values have been depth corrected to 4 cm, an expected depth in at least some surface pools of effluent which has leaked from adjacent settling pond dikes.

In cooperation with the Environmental Protection Agency, luminescence of phosphate processing wastes were measured with the FLD in the Lakeland, Florida area during January 1975. Effluents from several major phosphate processing plants were measured at the 486.1 nm Fraunhofer line on both clear and overcast days. Measurement layout for one of the phosphate plants is shown in figure 29. Table 17 shows luminescence counts (mean and standard deviation) and equivalent rhodamine WT concentration (ppb) as

Table 16. Luminescence of samples of phosphate processing effluent at six Fraunhofer lines in terms of rhodamine WT equivalency (source-detector and solar corrected; depth corrected to 4 cm). Effluent samples were collected from processing plants west of Mulberry, Florida. Reference samples were collected from rivers several tens of kilometres outside the phosphate area.

Sample	FRAUNHOFER WAVELENGTH (NANOMETERS)					
	396.8 (ppb)	422.7 (ppb)	386.1 (ppb)	518.4 (ppb)	589.0 (ppb)	656.3 (ppb)
Effluent 1	.35	.77	1.81	1.87	.67	.15
Effluent 2	.30	.74	1.23	1.12	.41	.09
Effluent 3	.30	.60	.91	1.00	.25	.05
Effluent 4	.50	.88	1.18	1.17	.25	.02
Effluent 5	.41	.77	1.10	1.09	.33	.12
Effluent 6	.37	.81	.98	1.00	.28	.09
Reference 17	.08	.12	.15	.15	.07	.04
Reference 18	.09	.14	.17	.23	.10	.02
Reference 19	.06	.11	.16	.16	.08	.03